EAT-2, a SAP-like adaptor, controls NK cell activation through phospholipase Cγ, Ca^{++}, and Erk, leading to granule polarization

Luis-Alberto Pérez-Quintero,[1,2] Romain Roncagalli,[1,3] Huaijian Guo,[1,2] Sylvain Latour,[4] Dominique Davidson,[1] and André Veillette[1,2,3]

[1]Laboratory of Molecular Oncology, Clinical Research Institute of Montréal, Montréal, Québec H2W 1R7, Canada
[2]Department of Medicine, McGill University, Montréal, Québec H3G 1Y6, Canada
[3]Department of Medicine, University of Montréal, Montréal, Québec H3T 1J4, Canada
[4]INSERM UMR 1163, Laboratory of Lymphocyte Activation and Susceptibility to EBV, Université Paris Descartes-Sorbonne Paris Cité, Institut Imagine, 75743 Paris, France

Ewing's sarcoma–associated transcript 2 (EAT-2) is an Src homology 2 domain–containing intracellular adaptor related to signaling lymphocytic activation molecule (SLAM)–associated protein (SAP), the X-linked lymphoproliferative gene product. Both EAT-2 and SAP are expressed in natural killer (NK) cells, and their combined expression is essential for NK cells to kill abnormal hematopoietic cells. SAP mediates this function by coupling SLAM family receptors to the protein tyrosine kinase Fyn and the exchange factor Vav, thereby promoting conjugate formation between NK cells and target cells. We used a variety of genetic, biochemical, and imaging approaches to define the molecular and cellular mechanisms by which EAT-2 controls NK cell activation. We found that EAT-2 mediates its effects in NK cells by linking SLAM family receptors to phospholipase Cγ, calcium fluxes, and Erk kinase. These signals are triggered by one or two tyrosines located in the carboxyl-terminal tail of EAT-2 but not found in SAP. Unlike SAP, EAT-2 does not enhance conjugate formation. Rather, it accelerates polarization and exocytosis of cytotoxic granules toward hematopoietic target cells. Hence, EAT-2 promotes NK cell activation by molecular and cellular mechanisms distinct from those of SAP. These findings explain the cooperative and essential function of these two adaptors in NK cell activation.

CORRESPONDENCE
André Veillette:
veillea@ircm.qc.ca

Abbreviations used: CRACC, CD2-like receptor-activating cytotoxic cell; EAT-2, Ewing's sarcoma-associated transcript 2; ERT, EAT-2–related transducer; iNK cell, immature NK cell; KI, knock-in; LAK, lymphokine-activated killer; mNK, mature NK cell; MTOC, microtubule-organizing center; NKP, NK cell precursor; NTB-A, NK-T-B-antigen; PLC, phospholipase C; PTK, protein tyrosine kinase; SAP, SLAM-associated protein; SH2, Src homology 2; SHIP, SH2 domain-containing inositol phosphatase; SLAM, signaling lymphocytic activation molecule.

NK cells are innate immune cells playing a critical role in protection against viruses and cancer cells (Raulet, 2003; Lanier, 2005; Bryceson and Long, 2008; Vivier et al., 2008). They also influence antigen-specific immune responses by regulating cells such as DCs and T cells. NK cell activation is controlled by stimulation of various activating and inhibitory receptors, which recognize ligands that may or may not be present on target cells. When activating signals predominate, NK cells kill target cells, primarily through natural cytotoxicity. They also secrete cytokines such as IFN-γ, which amplify the immune response by activating other immune cells.

The signaling lymphocytic activation molecule (SLAM)–associated protein (SAP) family is a group of intracellular adaptor molecules made up almost exclusively of a Src homology 2 (SH2) domain (Detre et al., 2010; Veillette, 2010; Cannons et al., 2011). In humans, it includes two members named SAP and Ewing's sarcoma-associated transcript 2 (EAT-2). A third member, EAT-2–related transducer (ERT), exists in mice but not in humans (Roncagalli et al., 2005). SAP is expressed in NK cells, T cells, and NK-T cells, whereas EAT-2 is found in NK cells and, at least in mice, DCs and macrophages. ERT is found only in mouse NK cells. The gene encoding SAP, *SH2D1A*, is mutated and inactivated in X-linked lymphoproliferative (XLP) syndrome, a human immunodeficiency characterized by an inability to cope with EBV infection. NK cells and CD8$^+$ T cells from XLP patients have defects in killing of EBV-infected B cells and activated immune cells, thereby

The Rockefeller University Press $30.00
J. Exp. Med. 2014 Vol. 211 No. 4 727-742
www.jem.org/cgi/doi/10.1084/jem.20132038

causing severe lymphoproliferative illnesses and lymphomas in these individuals.

Through their SH2 domain, SAP family adaptors interact with phosphorylated tyrosine-based motifs in the cytoplasmic domain of SLAM family receptors, which include SLAM, 2B4, Ly-9, CD84, NTB-A (NK-T-B-antigen; Ly108 in the mouse), and CD2-like receptor-activating cytotoxic cell (CRACC; Detre et al., 2010; Veillette, 2010; Cannons et al., 2011). SLAM family receptors are exclusively expressed on hematopoietic cells. Most are self-ligands, with the exception of 2B4, which interacts with CD48, another hematopoietic cell–restricted receptor. All SLAM family receptors bind SAP and EAT-2, except for CRACC, which binds only EAT-2.

The interaction of SAP with SLAM family receptors dictates whether these receptors stimulate or inhibit immune cell functions (Detre et al., 2010; Dong and Veillette, 2010; Veillette, 2010; Cannons et al., 2011). In the presence of SAP, SLAM family receptors mediate activating effects through a dual molecular mechanism (Parolini et al., 2000; Bottino et al., 2001; Dong et al., 2009, 2012; Kageyama et al., 2012; Zhao et al., 2012). On the one hand, SAP couples SLAM family receptors to tyrosine phosphorylation signals as a result of its ability to bind and activate the Src family protein tyrosine kinase (PTK) Fyn. On the other hand, SAP prevents the coupling of SLAM family receptors to inhibitory signals involving the lipid phosphatase SH2 domain–containing inositol phosphatase (SHIP) 1 and the protein tyrosine phosphatase SHP-1. At the cellular level, these two activities allow SAP to stabilize conjugate formation between the SAP-expressing lymphocytes and other hematopoietic cells (Qi et al., 2008; Dong et al., 2012). This feature likely explains why SAP is necessary for the ability of NK cells and $CD8^+$ T cells to kill abnormal hematopoietic cells (Parolini et al., 2000; Bottino et al., 2001; Dupré et al., 2005; Dong et al., 2009, 2012; Hislop et al., 2010; Palendira et al., 2011, 2012; Zhao et al., 2012).

Both SAP and EAT-2 are expressed in NK cells (Roncagalli et al., 2005). Whereas NK cells lacking either SAP or EAT-2 had partial defects in NK cell–mediated cytotoxicity toward abnormal hematopoietic cells, much more pronounced defects existed in NK cells lacking both adaptors (Dong et al., 2009, 2012). Hence, these two adaptors cooperate to promote NK cell–mediated killing. However, the mechanism by which EAT-2 mediates its function was not determined. It is unclear if EAT-2 triggers active biochemical signals during NK cell activation or if it functions solely by preventing the inhibitory function of SLAM family receptors. The mechanism by which EAT-2 generates the putative signals, as well as the nature of these signals, are also uncertain. Lastly, it is not established if EAT-2 enhances NK cell activation by promoting conjugate formation between NK cells and target cells, as is the case for SAP (Dong et al., 2012), or if it acts on another step of NK cell activation.

Herein, we elucidated these issues using a variety of genetic, biochemical, and imaging studies. We found that, in NK cells, EAT-2 induced signals and effects distinct from those evoked by SAP. These signals involved phospholipase C (PLC) γ, Ca^{2+} fluxes, and Erk activation. They were mediated by one or two tyrosines located in the C-terminal tail of EAT-2 but not in SAP. Unlike the situation of SAP, the EAT-2–induced signals not only promoted the activating function of SLAM family receptors but also prevented their inhibitory function. Moreover, EAT-2 did not stabilize conjugate formation between NK cells and target cells. Rather, it accelerated polarization of cytotoxic granules toward the target cells, as well as granule exocytosis. The ability of EAT-2 to trigger signals and effects distinct from those of SAP provides an explanation for the essential and cooperative function of these two adaptors in NK cell activation.

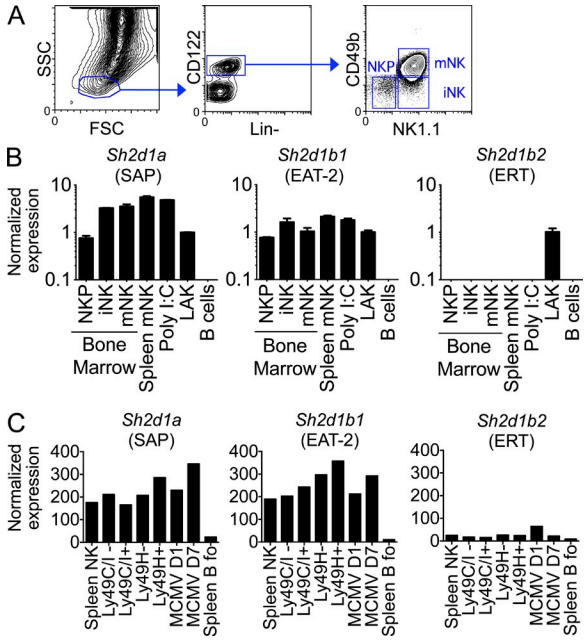

Figure 1. Expression of SAP family adaptors in various NK cell populations. (A) NKPs, iNK cells, and mNK cells were sorted from bone marrow of C57BL/6 mice by first gating on forward scatter channel (FSC)- and side scatter channel (SSC)-low cells and then on lineage $(Lin)^-$ $CD122^+$ cells. NKPs are $NK1.1^-$ $CD49b^-$, whereas iNK and mNK cells are $NK1.1^+$, $CD49b^-$, and $NK1.1^+$ $CD49b^+$, respectively. (B) RNAs from purified NK cell populations in bone marrow, spleen mNK, and splenic NK cells from poly I:C–primed mice (poly I:C), LAK cells, and splenic B cells were subjected to reverse transcription and real-time PCR with gene-specific primers for *Sh2d1a* (SAP), *Sh2d1b1* (EAT-2), *Sh2d1b2* (ERT), or *Gapdh*. Cross threshold (CT) values were normalized to *Gapdh* for each cell type and are relative to values for LAK cells. The resulting values (ΔCT) are shown. Mean values with error bars and standard deviations of duplicates from a representative experiment are shown. Shown is a representative of 4 independent experiments. (C) Normalized RNA expression for *Sh2d1a* (SAP), *Sh2d1b1* (EAT-2), and *Sh2d1b2* (ERT) in total, $Ly49C/I^+$, $Ly49C/I^-$, $Ly49H^+$, or $Ly49H^-$ resting splenic NK cells, or in NK cells from mice infected for 1 (D1) or 7 (D7) days with mouse cytomegalovirus (MCMV), were obtained from the Immgen consortium. Values for splenic follicular B cells (B fo) are shown as control. Details on data generation are available at www.immgen.org.

RESULTS

EAT-2 and SAP, but not ERT, are broadly expressed in NK cells

To help understand the relative contributions of SAP family members in NK cells, the expression patterns of the three

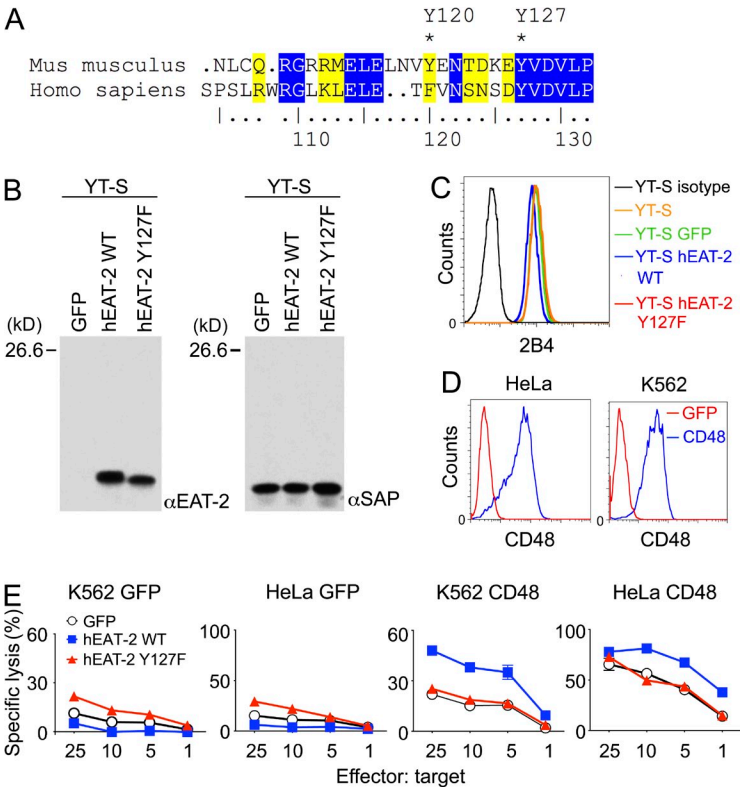

Figure 2. The unique C-terminal tyrosine of human EAT-2 is required for enhancement of NK cell–mediated cytotoxicity. (A) Sequence alignment of the C-terminal tail of mouse (*Mus musculus*) and human (*Homo sapiens*) EAT-2. The tail corresponds to residues 105 to 132 in the mouse protein. Identities are highlighted in blue, whereas similarities are highlighted in yellow. The positions of tyrosine 120 (Y120) and tyrosine 127 (Y127) in the mouse sequence are indicated by asterisks. For maximal alignment, gaps were introduced in sequences and are shown by dots. (B–E) WT or tyrosine 127-to-phenylalanine 127 (Y127F) human (h) EAT-2 was expressed in YT-S cells by retroviral infection. Cells expressing GFP alone were used as control. (B) Expression of EAT-2 and SAP was determined by immunoblotting of total cell lysates. Shown is a representative of at least 3 independent experiments. (C) Expression of 2B4 was determined by flow cytometry with anti-2B4 (mAb C1.7) or isotype control antibodies. Shown is a representative of at least 3 independent experiments. (D) Expression of CD48 on HeLa and K562 target cells, expressing GFP alone or in the presence of CD48, was examined by flow cytometry. Shown is a representative of at least 3 independent experiments. (E) Natural cytotoxicity toward HeLa or K562 target cells, expressing CD48 or not, was examined by incubating YT-S derivatives (effectors) with ^{51}Cr-labeled targets at the indicated effector-to-target ratios. Data are represented as percentage of maximal lysis. Standard deviations of duplicates are shown by error bars. Shown is a representative of 9 independent experiments.

members in the mouse were analyzed in various NK cell populations (Fig. 1). Real-time PCR analyses of RNA obtained from highly purified NK cell subsets showed that SAP (encoded by *Sh2d1a*) and EAT-2 (encoded by *Sh2d1b1*) were expressed at all stages of NK cell maturation, including NK cell precursors (NKPs), immature NK cells (iNK cells), and mature NK cells (mNK cells; Fig. 1, A and B). Lower levels of both adaptors were noted in NKPs, whereas higher amounts were observed in mNK cells. SAP and EAT-2 RNAs were also found in splenic NK cells from poly I:C–primed mice and lymphokine-activated killer (LAK) cells. In contrast, ERT (encoded by *Sh2d1b2*) was solely observed in LAK cells.

Complementary information was obtained from the ImmGen database (Fig. 1 C). Once again, SAP and EAT-2 RNAs were co-expressed in all NK cell subsets tested. The latter included Ly49C/I$^+$ and Ly49C/I$^-$ cells, which are educated or not by class I major histocompatibility complex molecules, respectively. They also included NK cells isolated at different times after infection with mouse cytomegalovirus. In contrast, little or no ERT RNA was found in all NK cell populations. Thus, SAP and EAT-2 were co-expressed at all stages of NK cell maturation and in all NK cell subsets. ERT was exclusively found in LAK cells.

Conserved C-terminal tyrosine is critical for activating function of human EAT-2

SAP mediates its activating signals via an arginine at position 78 (R78) in the SH2 domain, which binds and activates the Fyn kinase (Latour et al., 2001, 2003; Chan et al., 2003). This arginine is not present in EAT-2. Rather, EAT-2 possesses tyrosines in the region C-terminal to the SH2 domain, the so-called tail, which can undergo phosphorylation (Roncagalli et al., 2005). In mice and most other nonprimate species, the tail bears two tyrosines, tyrosine 120 (Y120) and tyrosine 127 (Y127; Fig. 2 A and not depicted). In contrast, in humans and other primates, it contains a single tyrosine, Y127.

To determine if the single C-terminal tyrosine of human EAT-2 was critical for its activating function, we generated polyclonal derivatives of the human NK cell line YT-S that expressed equivalent amounts of either WT or tyrosine 127-to-phenylalanine 127 (Y127F) human EAT-2 (Fig. 2 B). Parental YT-S cells express endogenous SAP and SLAM family receptor 2B4 but do not contain EAT-2 (Fig. 2, B and C). Cells were then tested for their capacity to mediate cytotoxicity toward HeLa or K562 target cells, expressing or not the ligand of 2B4, CD48 (Fig. 2, D and E). The ability of YT-S to kill targets expressing CD48 was greatly enhanced by expression of WT EAT-2. This effect was not seen when targets lacked CD48, implying that it was mediated by 2B4. It was also eliminated when Y127 of EAT-2 was mutated. Hence, the capacity of human EAT-2 to promote the activating function of 2B4 required the C-terminal tyrosine Y127.

Creation of mouse strain lacking C-terminal tyrosines of EAT-2

To ascertain the role of the two C-terminal tyrosines found in mouse EAT-2, we created a knock-in (KI) mouse in which Y120 and Y127 were mutated to phenylalanines (*Sh2d1b1*^{Y120,127F} mouse, hereafter called EAT-2 KI mouse). The vector depicted

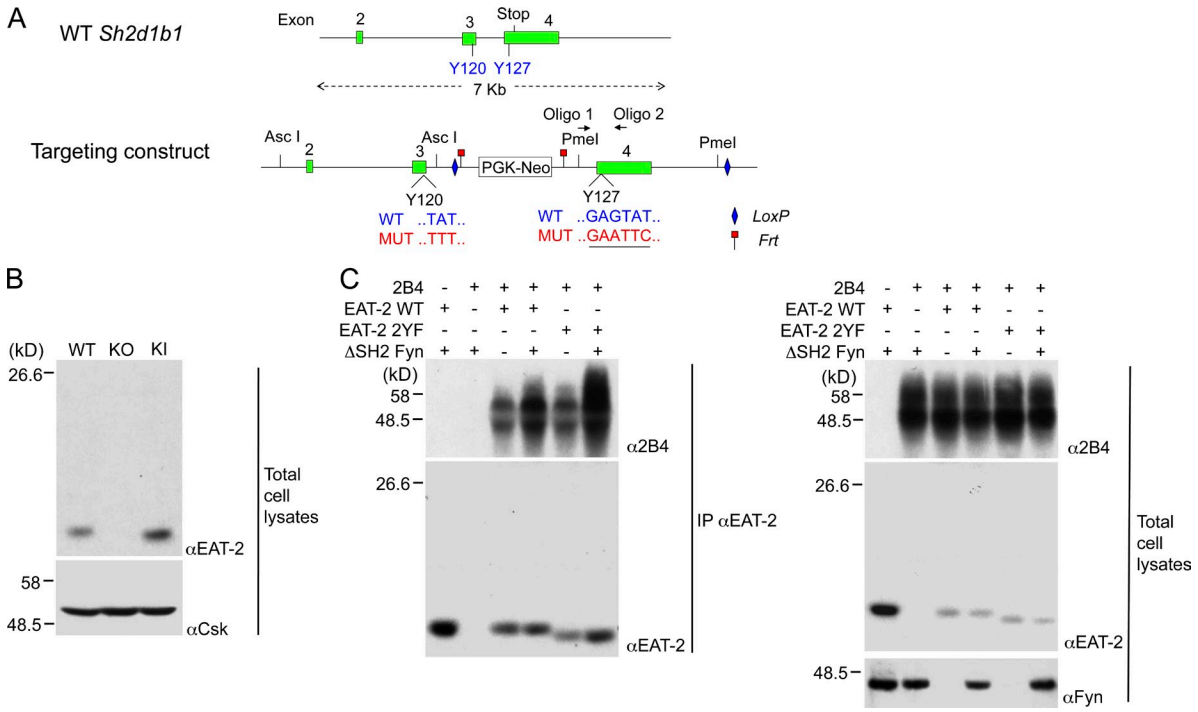

Figure 3. Generation of *Sh2d1b1*^{Y120,127F} mouse. (A) The exon-intron structure of the WT EAT-2-encoding gene in the mouse (*Sh2d1b1*) is shown at the top. Tyrosine 120 (Y120) is encoded by exon 3, whereas tyrosine 127 (Y127) is encoded by exon 4. The STOP codon is also contained in exon 4. The targeting construct used to create the *Sh2d1b1*^{Y120,127F} KI mouse is shown at the bottom. The 5′ arm contains exons 2 and 3. The WT codon for Y120, TAT, was replaced by the mutated (MUT) codon TTT. The 3′ arm bears exon 4. The WT codon for Y127, TAT, was replaced by TTC. An additional mutation, which does not change the amino-acid sequence, was created at codon 126 (GAG to GAA) to introduce a novel EcoRI site (GAATTC) for genomic screening. (B) Lysates of bone marrow–derived dendritic cells from WT, EAT-2–deficient (EAT-2 KO), and EAT-2 KI mice were probed by immunoblotting with the indicated antibodies. Shown is a representative of 3 independent experiments. (C) WT or Y120,127F (2YF) mouse EAT-2 was co-expressed with 2B4 in Cos-1 cells, in the absence or in the presence of an SH2 domain–deleted version (ΔSH2) of Fyn. EAT-2 was immunoprecipitated and its association with 2B4 was detected by immunoblotting. 2B4, EAT-2, and Fyn were detected in total cell lysates. Shown is a representative of 3 independent experiments.

in Fig. 3 A was used. Immunoblot analyses of lysates from bone marrow–derived DCs of these mice showed that the mutations did not destabilize the EAT-2 protein (Fig. 3 B). DCs were used for this study, as the amounts of protein needed for immunoblotting could only be obtained with LAK cells and these cells also express ERT. The available anti–EAT-2 antibodies recognize ERT. Mutation of the C-terminal tyrosines also did not affect the ability of EAT-2 to bind 2B4 (Fig. 3 C). Furthermore, it had no impact on NK cell development, as assessed by expression of CD27, CD11b, and various Ly49 receptors, or on the expression levels of SLAM family receptors CD48 and SAP (unpublished data), as reported for EAT-2 deficiency (Roncagalli et al., 2005; Dong et al., 2009, 2012).

C-terminal tyrosines are needed for dual function of EAT-2 in NK cells

The impact of the EAT-2 KI mutation on NK cell activation was examined (Fig. 4). First, purified ex vivo NK cells were tested for their ability to kill hematopoietic target cells (Fig. 4 A). In comparison to WT NK cells, EAT-2 KI NK cells displayed a reduced ability to kill the hematopoietic cell lines RMA-S (lymphoma) and YAC-1 (thymoma). This defect was analogous to that seen in NK cells from EAT-2–deficient (EAT-2 KO) mice (Dong et al., 2009, 2012). Second, NK cells were assessed for their aptitude to produce IFN-γ in response to target cells, using intracellular staining with anti–IFN-γ antibodies (Fig. 4 B). Once again, in comparison to WT NK cells, EAT-2 KI NK cells exhibited reduced production of IFN-γ in response to RMA-S and YAC-1. This defect was similar to the one observed in EAT-2 KO NK cells (Dong et al., 2009, 2012). However, there was no defect when cells were activated with PMA and ionomycin, which bypass NK cell receptors.

To address the function of SLAM family receptors, similar experiments were conducted using as targets the nonhematopoietic cell line B16 (melanoma), expressing or not ligands for individual SLAM family receptors (Fig. 4 C). When compared with WT NK cells, NK cells expressing the EAT-2 KI mutation had dramatically compromised NK cell activation when SLAM family ligands were expressed on B16. This was true for cells expressing the ligands of 2B4 (that is, CD48), CRACC, CD84, and Ly-9. The defects were similar to those observed in EAT-2–deficient NK cells. However, neither the KI mutation nor EAT-2 deficiency had any impact on the capacity of NK cells to kill B16 lacking SLAM family ligands (B16-GFP).

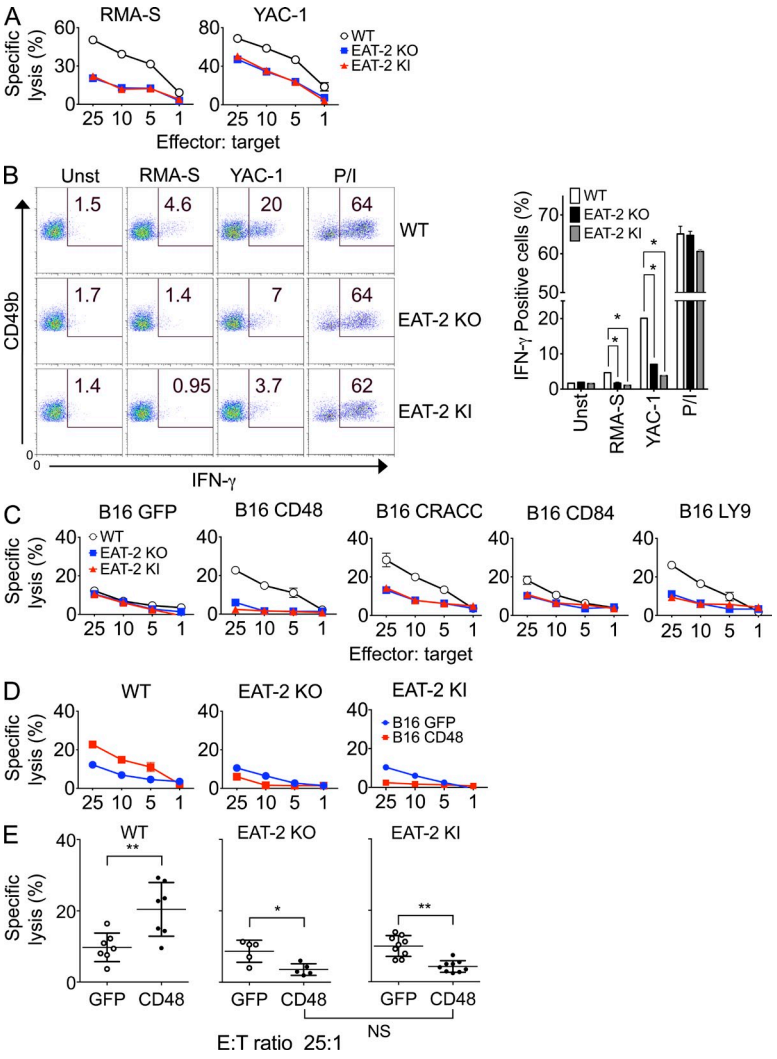

Figure 4. The C-terminal tyrosines are necessary for the dual function of mouse EAT-2 in NK cell activation. (A) Ex vivo splenic NK cells from poly I:C–primed mice were tested for their capacity to kill the hematopoietic target cells, RMA-S or YAC-1, at the indicated effector–to–target cell ratios. Data are represented as percentage of maximal lysis. Error bars show standard deviations of duplicates. Shown is a representative of 6 independent experiments. (B) Splenocytes from poly I:C–primed mice were tested for their ability to produce IFN-γ in the presence of RMA-S or YAC-1. Unstimulated cells (Unst) or cells stimulated with phorbol myristate acetate and ionomycin (P+I) were used as controls. NK cells were identified by gating on CD49b$^+$ TCR-β$^-$ cells. Percentages of IFN-γ$^+$ cells are shown. Representative dot plots are shown on the left, whereas a statistical analysis of duplicates is depicted on the right. Mean values with error bars and standard deviations of triplicates from a representative experiment are shown on the right. *, $P < 0.05$. Shown is a representative of 2 independent experiments. (C–E) Experiments were performed as in A, except that target cells were nonhematopoietic B16 cells expressing GFP alone or in combination with different SLAM family ligands. (C) NK cells were tested for cytotoxicity against various B16 derivatives. Mean values with error bars and standard deviations of duplicates from a representative experiment are shown. Shown is a representative of at least 4 experiments. (D) Cytotoxicity toward B16 cells expressing GFP alone or in combination with CD48 was analyzed in NK cells from each mouse. Shown is a representative of at least 5 independent experiments. (E) A graphic representation of cytotoxicity toward B16 cells expressing or not CD48 is shown for several independent mice of each genotype (WT, $n = 7$; KO, $n = 5$; KI, $n = 9$). The 25:1 effector-to-target (E:T) ratio was analyzed. Individual symbols represent individual mice. Mean values, standard deviations, and P-values are depicted. *, $P < 0.02$; **, $P < 0.002$. EAT-2 KO, EAT-2–deficient mice; EAT-2 KI, mice expressing Y120,127F EAT-2; NS, not significant ($P > 0.3$).

SAP family adaptors enhance NK cell activation by a dual mechanism (Dong et al., 2009, 2012; Kageyama et al., 2012; Zhao et al., 2012). They promote the activating function of SLAM family receptors and prevent their inhibitory function. In the case of SAP, activation, but not prevention of inhibition, is dependent on the signaling motif, R78 (Dong et al., 2012). To evaluate if this was also the case for EAT-2, we presented the data of Fig. 4 C in a different manner for a side-by-side comparison of the impact of engaging or not engaging 2B4 in the different mice (Fig. 4 D). To show reproducibility, data from multiple independent experiments are represented in Fig. 4 E. Engagement of 2B4 by CD48 enhanced killing of B16 by WT NK cells. In contrast, it suppressed cytotoxicity by EAT-2 KO NK cells. Surprisingly, it was also the case for EAT-2 KI NK cells.

Thus, the C-terminal tyrosines were needed for the ability of mouse EAT-2 to promote NK cell activation by SLAM family receptors. Unlike the situation of SAP, this putative signaling motif of EAT-2 was also required to prevent the inhibitory function of SLAM family receptors.

Tyrosines of EAT-2 trigger specific signals involving PLCγ, Ca^{2+}, and Erk

Previous reports suggested that EAT-2 may couple SLAM family receptors to a wide range of signals in NK cells involving Fyn, Lck, phosphatidyl inositol 3′ kinase (PI3′K), Akt, PLCγ, c-Cbl, and others (Morra et al., 2001; Tassi and Colonna, 2005; Calpe et al., 2006; Clarkson et al., 2007; Clarkson and Brown, 2009). However, whether EAT-2 or other effectors were responsible for these signals was not addressed genetically.

To identify the signals mediated by EAT-2 in human NK cells, YT-S cells expressing WT EAT-2 or not were stimulated with anti-2B4 antibodies. Then, a variety of biochemical signals was analyzed (Fig. 5). Immunoblotting of total cell lysates with anti-phosphotyrosine antibodies showed that expression of WT EAT-2 had no impact on the overall pattern of protein tyrosine phosphorylation induced by 2B4 stimulation (Fig. 5 A). WT EAT-2 also had no influence on tyrosine phosphorylation of 2B4 (Fig. 5 B). Likewise, it had no effect on tyrosine phosphorylation of Vav-1, a key target of SAP in NK cells (Fig. 5 C; Dong et al., 2012). Tyrosine phosphorylation

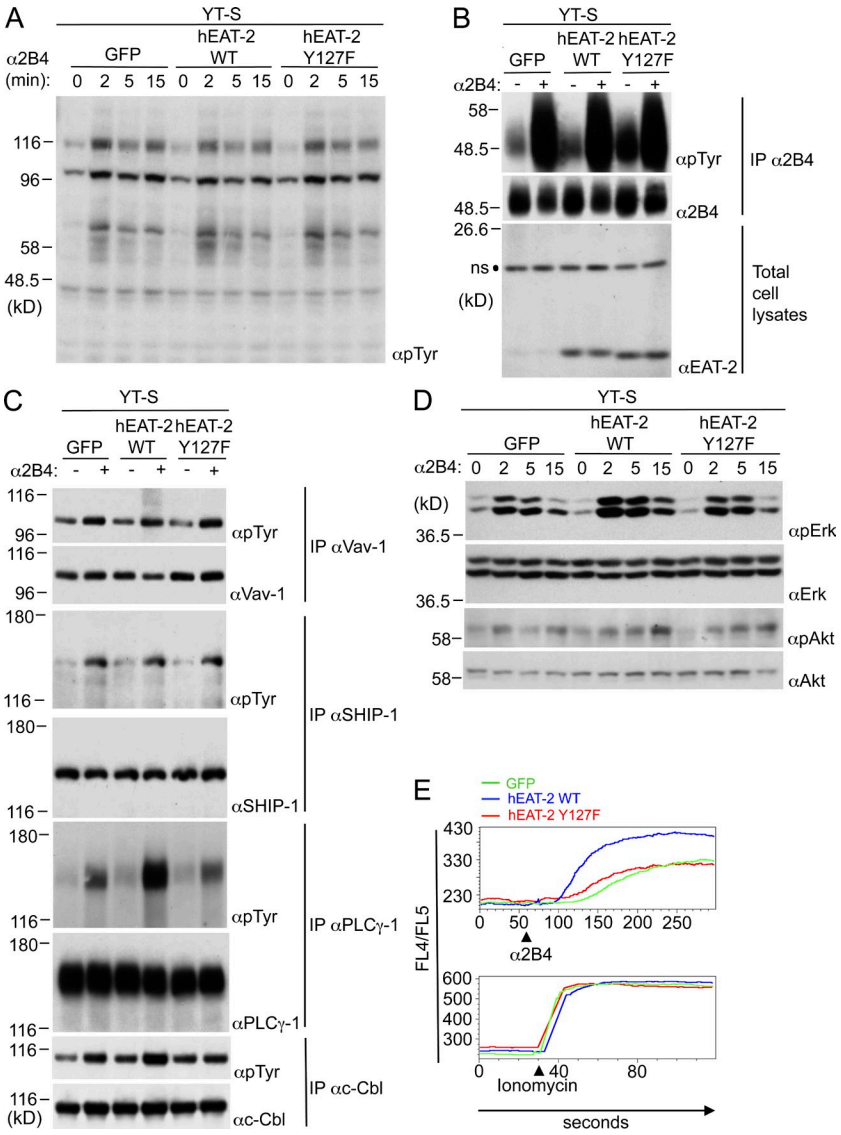

Figure 5. EAT-2 induces specific signals in NK cells. YT-S derivatives expressing GFP alone or in combination with WT or tyrosine 127-to-phenylalanine 127 (Y127F) human (h) EAT-2 were stimulated with anti-human 2B4 mAb C1.7 followed by the relevant secondary antibody. (A) Total cell lysates were probed by immunoblotting with anti-phosphotyrosine (pTyr) antibodies. Cells were stimulated for the indicated times with anti-2B4. Shown is a representative of 5 experiments. (B) 2B4 was recovered by immunoprecipitation and probed by immunoblotting with anti-pTyr antibodies, as specified in Materials and methods. Cells were stimulated for 5 min. ns: nonspecific cross-reactive protein. Shown is a representative of 3 experiments. (C) The indicated substrates were recovered by immunoprecipitation with substrate-specific antibodies and probed by anti-pTyr immunoblotting. Cells were stimulated for 2 min. Shown is a representative of at least 4 experiments. (D) Total cell lysates were probed by immunoblotting with antibodies recognizing Erk phosphorylated at threonine 202 and tyrosine 204 (pErk), or Akt phosphorylated at serine 473 (pAkt). Cells were stimulated for the indicated times. Shown is a representative of at least 5 experiments. (E) Cells were loaded with Indo-1 and Ca^{2+} fluxes were monitored over time by flow cytometry. Free intracellular Ca^{2+} was determined by the FL4/FL5 fluorescence ratio. Ionomycin was used as control. Arrows indicate time of addition of anti-2B4 or ionomycin. Shown is a representative of 8 experiments.

of SHIP-1 was also not affected. These observations suggested that, unlike SAP (Dong et al., 2012), EAT-2 was not triggering activation of kinases such as Fyn or Lck. If this were the case, EAT-2 would likely cause a global enhancement of 2B4-evoked protein tyrosine phosphorylation.

Nevertheless, WT EAT-2 caused a prominent augmentation (approximately fivefold) of 2B4-triggered PLCγ-1 tyrosine phosphorylation. PLCγ-1 is the predominant PLCγ isoform expressed in YT-S cells and is also highly expressed in normal human NK cells (Ting et al., 1992). It also provoked a small increase (less than twofold) in c-Cbl tyrosine phosphorylation. In keeping with the effect on PLCγ-1, cells expressing WT EAT-2 also displayed augmented 2B4-triggered Erk activation and Ca^{2+} fluxes, the two downstream effectors of PLCγ (Fig. 5, D and E). No effect was seen on activation of Akt, suggesting that PI3′K was not activated (Fig. 5 D). Importantly, these various effects of EAT-2 were completely eliminated by the Y127F mutation, implying that they were mediated by the C-terminal tyrosine (Fig. 5, C–E).

Next, we ascertained whether EAT-2 was mediating similar signals in mouse NK cells (Fig. 6). To this end, WT, EAT-2 KI, and EAT-2 KO NK cells were stimulated with anti-2B4 antibodies and tyrosine phosphorylation of Vav-1 and SHIP-1 was first examined (Fig. 6 A). In keeping with the data with YT-S cells, EAT-2 KI or EAT-2 KO NK cells displayed no defect in the ability of 2B4 to enhance tyrosine phosphorylation of these targets. This was unlike SAP deficiency, which abolished 2B4-triggered tyrosine phosphorylation of Vav-1 (Dong et al., 2012). Surprisingly, no detectable tyrosine phosphorylation of PLCγ-2, the major isoform of PLCγ expressed in mouse NK cells (Tassi et al., 2005; Caraux et al., 2006; Regunathan et al., 2006), was seen upon engagement of 2B4. Moreover, triggering of 2B4 did not enhance tyrosine phosphorylation of PLCγ-2 in response to stimulation of CD16 (Fig. 6 B). Likewise, stimulation of 2B4 alone failed to induce Ca^{2+} fluxes (Fig. 6 C). These findings indicated that the full spectrum of 2B4-triggered signals was not evoked in normal

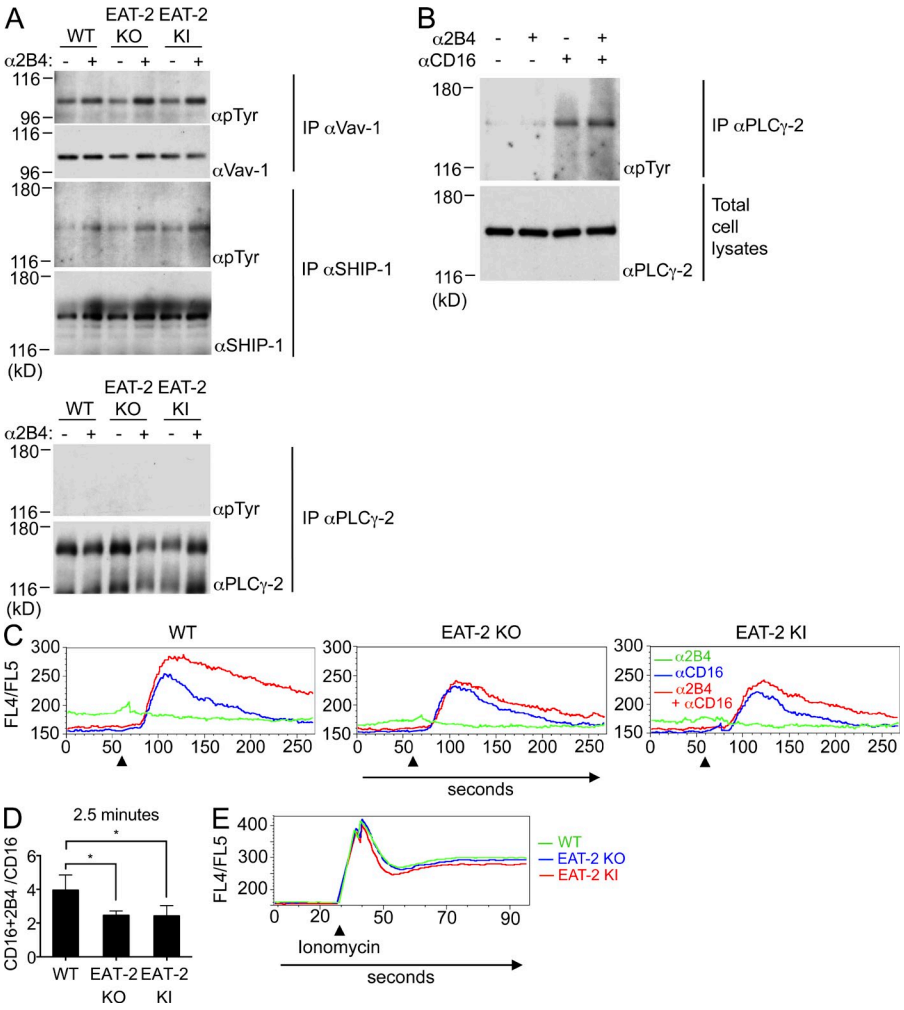

Figure 6. 2B4 signaling in *Sh2d1b1*^{Y120,127F} mouse. (A) IL-2–expanded NK cells from the indicated mice were stimulated or not for 2 min with anti–mouse 2B4 mAb 2B4 and the relevant secondary antibody. Tyrosine phosphorylation of the indicated substrates was examined as detailed for Fig. 5 C. Shown is a representative of 2–6 experiments. (B) NK cells from WT mice were stimulated or not for 2.5 min with antibodies against 2B4, CD16, or both. Tyrosine phosphorylation of PLCγ-2 was analyzed as detailed for A. (C–E) NK cells from the indicated mice were loaded with Indo-1 and stimulated with anti-2B4 alone, anti-CD16 alone, or a combination of anti-2B4 and anti-CD16. Ca^{2+} fluxes were examined as detailed for Fig. 5 E. A representative experiment is shown in C. Arrowheads indicate time of addition of antibodies. The ratios of increased Ca^{2+} levels over baseline for anti-CD16 + anti-2B4 over anti-CD16 alone were calculated at 2.5 min. Mean values with error bars and standard deviations from three independent experiments are shown in D. *, $P < 0.05$. NK cells were also stimulated with ionomycin and Ca^{2+} fluxes were examined (E). Arrowheads indicate time of addition of ionomycin. EAT-2 KO, EAT-2–deficient mice; EAT-2 KI, mice expressing Y120,127F EAT-2. Shown is a representative of 3 experiments.

mouse NK cells, in comparison with the human NK cell line YT-S. This may not be surprising, as the functional impact of engagement of activating receptors in primary immune cells is frequently weaker than in cell lines. This presumably reflects constraints on the signals emanating from activating receptors in primary cells. Nonetheless, stimulation of 2B4 on WT NK cells potentiated Ca^{2+} fluxes induced by the activating receptor CD16. Importantly, this enhancement was severely attenuated in EAT-KO and EAT-2 KI NK cells. A quantitation of data from three independent experiments is depicted in Fig. 6 D. All cells responded equally to ionomycin (Fig. 6 E).

PLCγ-2 is critical for the activating function of multiple NK cell receptors, including SLAM family receptors (Tassi et al., 2005; Caraux et al., 2006; Regunathan et al., 2006; Dong et al., 2012). To determine which downstream effectors of PLCγ were critical for the function of EAT-2, we analyzed the impact of prevention of Ca^{2+} fluxes, Erk activation, or both (Fig. 7 A). YT-S cells were incubated with the chelator

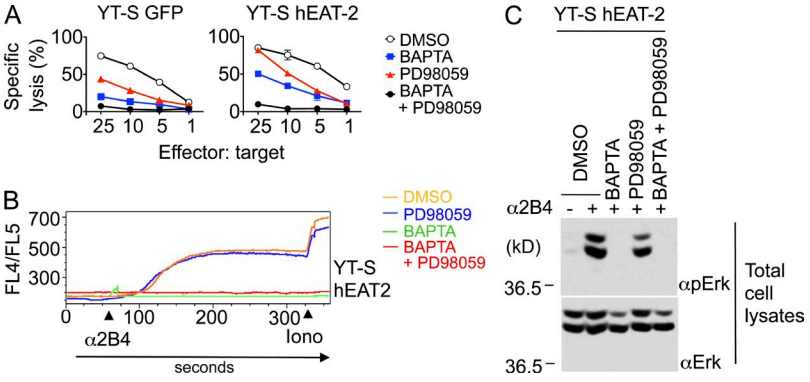

Figure 7. Role of calcium fluxes and Erk activation in EAT-2–mediated function. YT-S cells expressing GFP alone or in the presence of WT human (h) EAT-2 were preincubated for 30 min with BAPTA-AM (BAPTA), PD98059, or both. Cells exposed to DMSO alone were used as control. (A) Cytotoxicity toward K562 cells expressing CD48 was examined. Shown is a representative of 2 experiments. (B) 2B4-triggered Ca^{2+} fluxes were evaluated, as detailed for Fig. 5 E. Shown is a representative of 2 experiments. (C) 2B4-induced Erk activation was ascertained, as outlined for Fig. 5 D. Shown is a representative of 2 experiments.

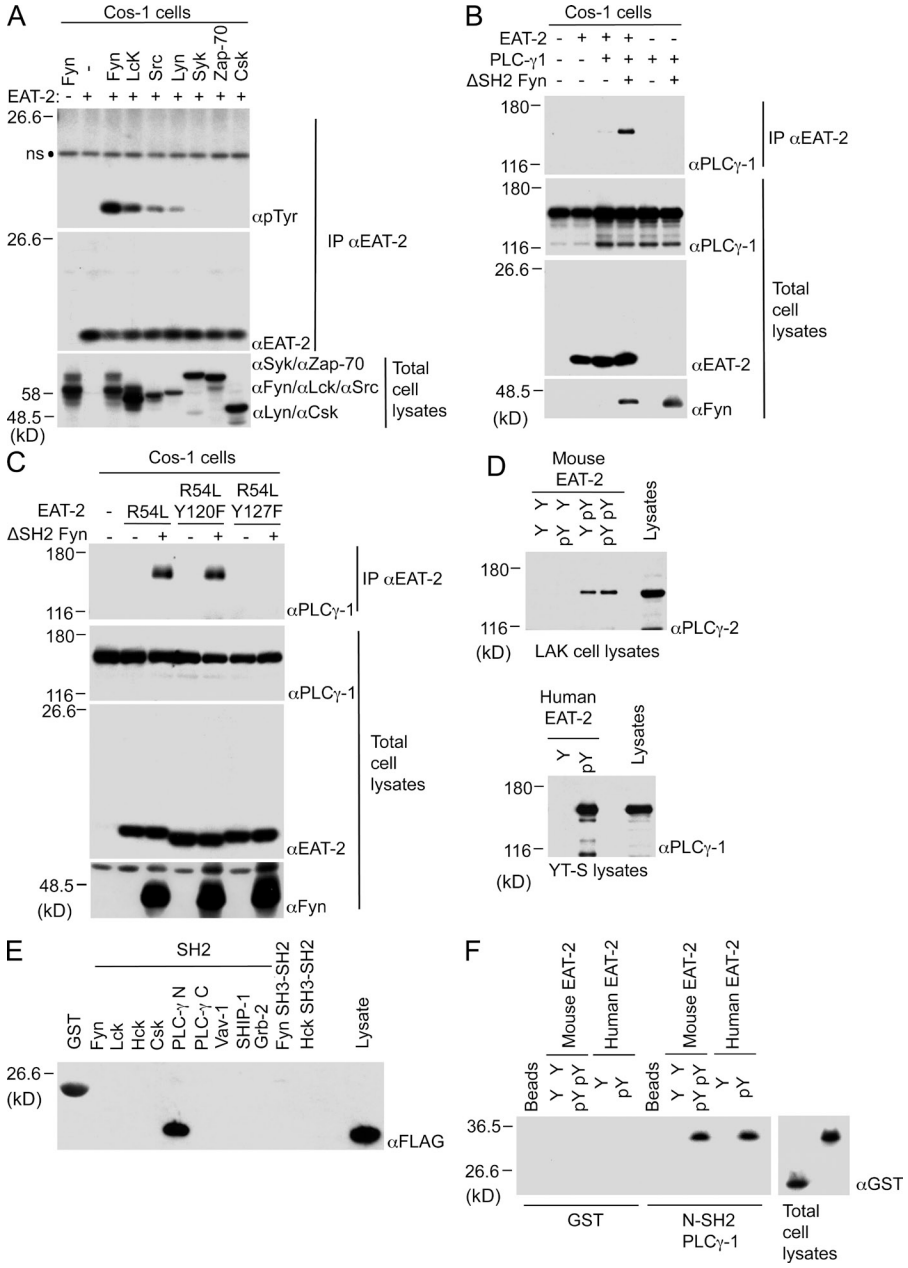

Figure 8. Phosphorylated tyrosine 127 of EAT-2 binds the N-terminal SH2 domain of PLCγ. (A) Mouse EAT-2 was co-expressed in Cos-1 cells in the presence of the indicated PTKs. EAT-2 was recovered by immunoprecipitation and probed by anti-phosphotyrosine (pTyr) immunoblotting. ns: nonspecific cross-reactive protein. Shown is a representative of 3 independent experiments. (B) Mouse EAT-2 was co-expressed with PLCγ-1 in Cos-1 cells, in the absence or in the presence of an SH2 domain–deleted version (ΔSH2) of Fyn. EAT-2 was immunoprecipitated and its association with PLCγ-1 was detected by immunoblotting. Shown is a representative of 2 independent experiments. (C) The experiment was performed as detailed for B, except that a variant of mouse EAT-2 carrying an inactivating mutation in the SH2 domain (arginine 54-to-leucine 54; R54L), in the absence or the presence of additional tyrosine 120-to-phenylalanine 120 (Y120F) or tyrosine 127-to-phenylalanine 127 (Y127F) mutations, was used. Shown is a representative of 2 independent experiments. (D) Immobilized synthetic peptides corresponding to the C-terminal tail of mouse or human EAT-2, phosphorylated or not at Y120, Y127, or both, were incubated with lysates from LAK cells or YT-S cells. Binding to PLCγ-2 or PLCγ-1 was detected by immunoblotting. Shown is a representative of 4 independent experiments. (E) Glutathione-S-transferase (GST) fusion proteins encompassing the indicated domains were incubated with lysates of HeLa cells expressing a FLAG-tagged version of EAT-2 in the presence of an SH2 domain–deleted version (ΔSH2) of Fyn. Binding to EAT-2 was detected by immunoblotting with anti-FLAG antibodies. Note that in the first lane, the GST protein cross-reacts with the anti-FLAG antibody. Shown is a representative of 2 experiments. (F) Immobilized EAT-2 peptides corresponding to the C-terminal tail of mouse or human EAT-2, phosphorylated or not at Y120, Y127, or both, were incubated with bacterial lysates expressing GST alone or in combination with the N-terminal SH2 domain (N-SH2) of PLCγ-1. After extensive washes, binding was detected by immunoblotting with anti-GST antibodies. Shown is a representative of 2 experiments.

of Ca^{2+} BAPTA-AM (1,2-bis(2-aminophenoxy)ethane-N,N,N′,N′-tetraacetic acid tetrakis(acetoxymethyl ester)), the MEK1 inhibitor PD98059, or both. BAPTA-AM or PD98059 alone resulted in a partial inhibition of cytotoxicity toward K562 cells expressing CD48. A more pronounced effect was seen when BAPTA-AM and PD98059 were combined. These effects were seen whether YT-S expressed EAT-2 or not, in keeping with the idea that multiple activating receptors are using these effectors.

As expected, BAPTA-AM also fully prevented 2B4-evoked Ca^{2+} fluxes (Fig. 7 B). Surprisingly, it also abolished 2B4-triggered Erk activation (Fig. 7 C). In contrast, PD98059 had only a small inhibitory impact on 2B4-induced Erk activation. The latter two findings suggested that Ca^{2+} fluxes, rather than MEK1, were primarily responsible for Erk activation in response to 2B4.

Therefore, unlike earlier proposals that EAT-2 triggers a broad range of signals in NK cells, EAT-2 induced a specific

subset of signals in response to 2B4 engagement. In YT-S cells, these signals included tyrosine phosphorylation of PLCγ, Ca^{2+} fluxes, and Erk activation. In mouse NK cells, they were limited to an enhancement of Ca^{2+} fluxes triggered by CD16. All these responses were strictly dependent on the C-terminal tyrosines of EAT-2.

Phosphorylated Y127 of EAT-2 interacts with the N-terminal SH2 domain of PLCγ

Next, the molecular mechanism by which EAT-2 coupled to PLCγ was evaluated. First, we ascertained which PTK was mediating tyrosine phosphorylation of EAT-2 (Fig. 8 A). Co-transfection experiments in Cos-1 cells showed that only the Src family kinases Fyn and, to a lesser extent, Lck, Src, and Lyn were able to induce tyrosine phosphorylation of EAT-2. Then, we tested whether EAT-2 was able to associate with full-length PLCγ in intact cells (Fig. 8, B and C). cDNAs encoding mouse EAT-2, PLCγ-1, and Fyn were co-transfected in cells (Fig. 8 B). When Fyn was expressed, there was prominent co-immunoprecipitation of EAT-2 with PLCγ-1. A much less extensive association was observed when Fyn was not expressed, implying that the interaction was mediated by Fyn-dependent tyrosine phosphorylation. To ensure that the interaction was due to binding of phosphorylated EAT-2 to PLCγ-1, rather than binding of EAT-2 to phosphorylated PLCγ-1, similar experiments were performed using EAT-2 polypeptides mutated at a residue critical for phosphotyrosine binding by the SH2 domain (arginine 54-to-leucine 54; R54L mutation; Morra et al., 2001) in the absence or the presence of additional mutations of the C-terminal tyrosines (Fig. 8 C). Y127 of EAT-2, but not Y120 or an intact SH2 domain, was required for the EAT-2–PLCγ-1 interaction.

To show directly that binding was dependent on phosphorylation of Y127, synthetic peptides corresponding to the C terminus of mouse EAT-2, phosphorylated or not at Y120, Y127, or both, were incubated with lysates from mouse LAK cells (Fig. 8 D). EAT-2 peptides phosphorylated at Y127, alone or in combination with Y120, bound to PLCγ-2. However, peptides phosphorylated at Y120 alone or not phosphorylated did not bind. A peptide encompassing the C-terminal tail of human EAT-2 phosphorylated at Y127, but not a nonphosphorylated version, also bound to PLCγ-1, as reported previously (Clarkson and Brown, 2009).

We also analyzed the ability of immobilized fusion proteins bearing the N-terminal or C-terminal SH2 domain of PLCγ-1 to bind mouse EAT-2, which was expressed in cells in combination with Fyn to enable phosphorylation of EAT-2 (Fig. 8 E). Unfortunately, the N-terminal domain from PLCγ-2 was not soluble when produced in bacteria (unpublished data). As controls, SH2 domains of Fyn, Lck, Hck, Csk, Vav-1, SHIP-1, and Grb-2, as well as combined SH3 and SH2 domains of Fyn and Hck, were tested. Only the N-terminal SH2 domain of PLCγ-1 interacted with EAT-2. Unlike previously reported (Clarkson et al., 2007), there was no binding of the Fyn SH2 domain to EAT-2.

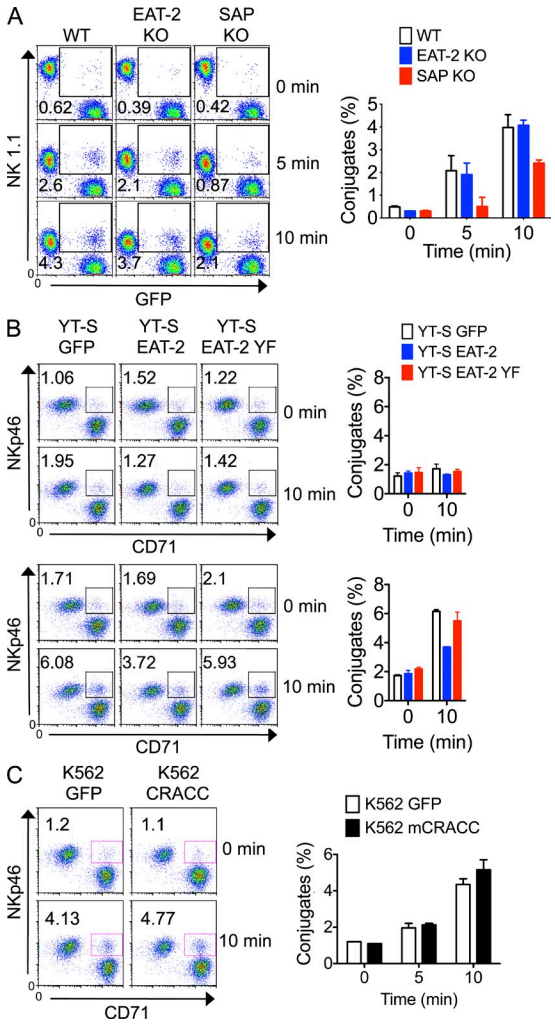

Figure 9. EAT-2 does not promote conjugate formation. (A) IL-2–expanded NK cells from WT, EAT-2–deficient (EAT-2 KO), or SAP-deficient (SAP KO) mice were labeled with PE-Cy7–conjugated anti-NK1.1 and incubated with RMA-S cells expressing GFP for the indicated times at 37°C. Conjugate formation was analyzed by flow cytometry. A representative experiment is shown on the left. Percentages of conjugate formation are shown at the bottom left of each dot plot. Mean values with error bars and standard deviations of duplicates from a representative experiment are shown on the right. Shown is a representative of 3 experiments. (B) YT-S cells expressing GFP alone or in the presence of EAT-2 WT or Y127F were labeled with Alexa Fluor 647–coupled anti-CD335 (NKp46). They were then incubated for the indicated times with K562 cells expressing CD48 (bottom) or not (top) and labeled with PE-coupled anti-CD71. Conjugate formation was analyzed as detailed for A. Percentages of conjugates are shown at the top left of each dot plot. Mean values with error bars and standard deviations of duplicates from a representative experiment are shown on the right. Shown is a representative of 3 experiments. (C) YT-S cells expressing mouse CRACC and EAT-2 were incubated with K562 cells expressing GFP alone or with mouse CRACC. Conjugate formation was analyzed as detailed for B. Mean values with error bars and standard deviations of duplicates from a representative experiment are shown below. Shown is a representative of 3 experiments.

Lastly, we tested the capacity of immobilized human or mouse EAT-2 peptides, phosphorylated or not at the C-terminal tyrosines, to bind the SH2 domain of PLCγ-1 (Fig. 8 F).

Phosphorylated EAT-2 peptides from human or mouse, but not unphosphorylated peptides, interacted with the SH2 domain of PLCγ-1. No interaction was seen with GST alone.

These data implied that, upon phosphorylation by Src family kinases, EAT-2 directly associated with PLCγ. This association was mediated by Y127 of EAT-2 and the N-terminal SH2 domain of PLCγ.

Unlike SAP, EAT-2 does not promote conjugate formation

NK cell–mediated cytotoxicity involves several steps (Orange, 2008). The initiation phase enables formation of stable conjugates between NK cells and target cells. SAP plays a key role during this phase (Dong et al., 2012). This is followed by the effector phase, which sequentially involves: (1) actin polymerization at the area of contact between NK cells and target cells, at the so-called NK cell synapse, (2) polarization of microtubule-organizing center (MTOC) and cytotoxic granules toward the NK cell synapse, (3) release of cytotoxic granules toward target cells, and (4) target cell killing.

To test if EAT-2 promoted the initiation phase, conjugate formation was evaluated using mouse NK cells lacking EAT-2 (Fig. 9 A). NK cells from WT, EAT-2 KO, or SAP KO mice were incubated with RMA-S cells, and conjugate formation was monitored. Whereas SAP deficiency resulted in compromised conjugate formation, loss of EAT-2 had no impact on this response. The impact of EAT-2 on conjugate formation was also ascertained in the YT-S system (Fig. 9 B). Compared with YT-S cells lacking EAT-2, cells expressing EAT-2 did not exhibit enhanced conjugate formation with K562 cells expressing CD48. In fact, even though EAT-2 promoted NK cell cytotoxicity (Fig. 2 E), it caused a reduction of conjugate formation with these targets (Fig. 9 B). This was seen at multiple time points (unpublished data). This effect was not seen in NK cells expressing EAT-2 Y127F. The latter finding implied that this effect was not simply a result of displacement of SAP from 2B4 due to EAT-2 overexpression but perhaps related to an inhibitory effect of EAT-2 signaling on adhesion.

We also examined the impact of CRACC on conjugate formation (Fig. 9 C). CRACC is a member of the SLAM family that interacts with EAT-2 but not SAP (Tassi and Colonna, 2005; Cruz-Munoz et al., 2009). Being a self-ligand, it is triggered when CRACC is expressed on target cells. When CRACC was expressed with EAT-2 in YT-S cells, it did not augment conjugate formation with K562 cells expressing CRACC. This was despite the fact that CRACC augmented killing of K562 cells expressing CRACC (Cruz-Munoz et al., 2009). We concluded that, unlike SAP, EAT-2 did not enhance conjugate formation with target cells.

EAT-2 stimulates granule polarization by way of Y127 and Ca^{2+} fluxes

To ascertain whether EAT-2 was promoting the effector phase, events occurring in conjugates of YT-S cells with K562 cells expressing CD48 were visualized by confocal microscopy (Fig. 10). YT-S, rather than primary NK cells, were chosen for these studies, as they are more homogeneous and easier to analyze by confocal microscopy. Phalloidin staining highlighted polymerized actin, whereas staining with anti-tubulin or anti-perforin antibodies identified MTOCs and cytotoxic granules, respectively (Fig. 10 A). Using this approach, various stages in the effector phase were identified (Fig. 10 B). Stage 0 corresponds to conjugates in which actin is not polymerized, and MTOC and granules are not polarized toward the synapse. Stage 1 represents conjugates in which polymerized actin, but not MTOC and granules, accumulates at the synapse. Stage 2 indicates conjugates where MTOC and granules have partially migrated toward the synapse. And stage 3 shows conjugates in which the MTOC and granules have fully migrated toward the synapse.

Comparison of YT-S cells expressing WT EAT-2 or not showed that EAT-2 augmented the proportions of conjugates exhibiting fully polarized (stage 3) or partially polarized (stage 2) MTOC and granules (Fig. 10 C). Conversely, it reduced the proportions of conjugates lacking MTOC or granule polarization (stage 1), or devoid of actin polymerization (stage 0). Such effects were not seen in YT-S cells expressing Y127F EAT-2. These data were statistically validated by correlation coefficient (r) analysis. Importantly, the enhancement of polarization by WT EAT-2 was seen even after a correction was made for the reduction of conjugate formation (Fig. 10 D). This implied that the increase in stages 2 and 3 conjugates was not simply due to a reduction of the stability of stages 0 and 1 conjugates but rather reflected a true acceleration of polarization.

To determine which downstream effectors of EAT-2 were mediating these effects, the impact of BAPTA-AM and PD98059 was examined (Fig. 10 E). BAPTA-AM alone, but not PD98059 alone, caused a marked increase in stage 0 conjugates, coupled to a decrease in stage 1, 2, and 3 conjugates. The combination of BAPTA-AM and PD98059 had effects similar to those of BAPTA-AM alone. Of note, these effects were seen not only in YT-S cells expressing WT EAT-2 but also in those expressing GFP alone. This finding indicated that Ca^{2+} fluxes were generally required for granule polarization, even in the absence of EAT-2.

Although microscopic analyses of primary mouse NK cells are challenging, we wanted to obtain support for the idea that EAT-2 signaling also promoted granule polarization in the mouse system (Fig. 10 F). To this end, we analyzed CD107a externalization, a consequence of degranulation, in NK cells from WT, EAT-2 KO, or EAT-2 KI mice. Compared with WT NK cells, NK cells from EAT-2 KO or EAT-2 KI mice displayed reduced exposure of CD107a in response to RMA-S targets. However, CD107a exposure in response to PMA and ionomycin was not affected. Therefore, EAT-2 promoted MTOC and granule polarization toward the NK cell synapse. This effect required Y127 and was mediated by the ability of EAT-2 to enhance Ca^{2+} fluxes.

DISCUSSION

To gain insight into the respective roles of EAT-2 and SAP in NK cells, their expression patterns in various NK cell

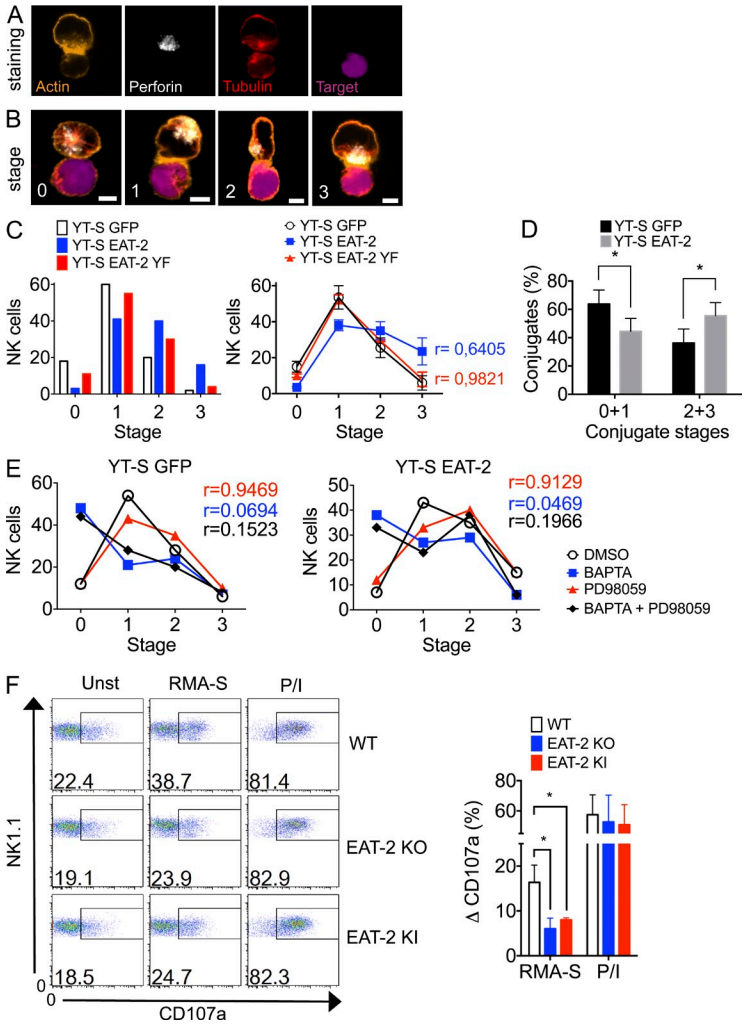

Figure 10. EAT-2 enhances granule polarization and exocytosis. (A) YT-S cells and CellTrace violet–loaded K562 cells were stained with phalloidin (actin), anti-perforin, and anti-tubulin. Conjugates were then analyzed by confocal microscopy. Individual stainings for a representative conjugate are shown. Scale bars are shown in B. Shown is a representative of 4 experiments. (B) Stained conjugates were categorized into different stages to describe progression of cytotoxicity, as detailed in the Methods section. Conjugates representative of each stage are shown. Bars, 5 µm. (C) YT-S cells expressing GFP alone or in combination with WT EAT-2 or tyrosine 127-to-phenylalanine 127 (Y127F) EAT-2 were incubated for 10 min with K562 cells expressing CD48. They were then stained as described for A and percentages of YT-S cells (NK cells) at each stage of cytotoxicity were determined. At least 100 conjugates were analyzed for each cell type. A bar graph representation of one experiment is shown on the left. A correlation coefficient (*r*) analysis between YT-S GFP cells and YT-S cells expressing WT or Y127F EAT-2 for 2 independent experiments is shown on the right. Mean values with standard deviations are shown. Shown is a representative of 2 experiments. (D) Data from C were corrected after assuming that the reduced conjugate formation in cells expressing EAT-2 observed in Fig. 9 B occurred only for stage 0 and 1 conjugates. Mean values with error bars and standard deviations of four independent experiments are shown. *, $P < 0.05$. (E) This experiment was performed as detailed for C, except that cells were preincubated with BAPTA-AM (BAPTA), PD98059, or both. Cells exposed to DMSO alone were used as control. Shown is a representative of 2 independent experiments. (F) Splenocytes from poly I:C–primed mice were incubated in the presence of RMA-S and tested by flow cytometry for their ability to up-regulate CD107a expression at the surface. Unstimulated cells (Unst) or cells stimulated with phorbol myristate acetate and ionomycin (P/I) were used as controls. NK cells were identified by gating on NK1.1$^+$ TCR-β$^-$ cells. Representative dot plots are shown on the left, whereas a statistical analysis of three experiments is depicted on the right. On the left, percentages of CD107a$^+$ cells are shown. On the right, values for unstimulated cells are subtracted from those of stimulated cells. Mean values with standard deviations are shown. *, $P \leq 0.02$. Shown is a representative of 3 independent experiments. EAT-2 KO, EAT-2–deficient mice; EAT-2 KI, mice expressing Y120,127F EAT-2.

populations were examined in the mouse. These studies showed that EAT-2 and SAP were co-expressed at all stages of NK cell differentiation and in all mNK cells. They also implied that EAT-2 and SAP might need to complement each other in all subsets of NK cells. In contrast, the third SAP family adaptor in the mouse, ERT, was detected only in LAK cells. It was not found in any freshly isolated NK cell population. The latter finding was in agreement with earlier studies showing that ex vivo NK cells from mice lacking ERT had no appreciable defect (Wang et al., 2010).

To elucidate the mechanism by which EAT-2 cooperates with SAP to promote NK cell activation, we focused on its C-terminal tyrosines. These tyrosines are not present in SAP and can undergo phosphorylation in NK cells (Roncagalli et al., 2005). Comparison of the EAT-2 sequence from several species showed that, in humans and other primates, the C-terminal tail contains only one tyrosine, Y127. In contrast, in most other species including mice, the tail encompasses two tyrosines, Y120 and Y127.

Overexpression studies of EAT-2 previously indicated that the tyrosines of EAT-2 were required for EAT-2 to suppress NK cell activation (Roncagalli et al., 2005). However, subsequent studies demonstrated that EAT-2 exhibits distinct functions whether target cells were hematopoietic or nonhematopoietic in origin. In the presence of hematopoietic target cells, EAT-2 is a positive regulator of NK cell activation (Dong et al., 2009, 2012). This correlates with the fact that only hematopoietic cells express ligands for SLAM family receptors, and is the predominant function of EAT-2 in NK cells.

To address the roles of the C-terminal tyrosines in this function, human and mouse EAT-2 polypeptides carrying or lacking these tyrosines were expressed in NK cells. Expression of human EAT-2 in the NK cell line YT-S showed that Y127 was absolutely needed for the capacity of human EAT-2 to

promote NK cell–mediated cytotoxicity in response to target cells expressing the ligand of 2B4. Likewise, creation of a KI mouse mutant expressing Y120,127F EAT-2 revealed that the tyrosines were required for the ability of mouse EAT-2 to augment NK cell cytotoxicity and IFN-γ production in response to targets expressing the ligand of 2B4, Ly-9, CD84, or CRACC. The loss of function caused by the tyrosine mutations was not due to reduced expression of EAT-2 or diminished association with SLAM family receptors. Rather, it was related to a compromised ability to mediate activating signals.

Biochemical studies in YT-S cells showed that human EAT-2 coupled 2B4 to specific signals involving PLCγ and its downstream effectors, Ca^{2+} fluxes and Erk. These signals were strictly reliant on Y127. There was no impact on other characterized 2B4-triggered tyrosine phosphorylation substrates, including 2B4 itself, Vav-1, and SHIP-1 (Chen et al., 2004). Moreover, there was no influence on Akt activation. A small increase in c-Cbl tyrosine phosphorylation was seen, although its mechanism and functional impact remain to be clarified. As c-Cbl is a ubiquitin ligase involved in signal termination (Thien and Langdon, 2005), c-Cbl tyrosine phosphorylation might be part of a negative feedback mechanism aimed at terminating the function of EAT-2.

Analyses of NK cells from EAT-2–deficient mice showed that, unlike SAP (Dong et al., 2012), EAT-2 did not promote tyrosine phosphorylation of Vav-1. However, in keeping with the effects of human EAT-2 in YT-S cells, mouse EAT-2 augmented the ability of 2B4 to enhance CD16-triggered Ca^{2+} fluxes. This effect was diminished when the C-terminal tyrosines were mutated. Although we were unable to detect tyrosine phosphorylation of PLCγ in mouse NK cells, these observations supported the idea that, by way of the C-terminal tyrosines, mouse EAT-2 was also coupling SLAM family receptors to the PLCγ pathway. It is possible that PLCγ was activated upon 2B4 triggering in mouse NK cells, but was not undergoing tyrosine phosphorylation. Alternatively, it is plausible that the extent of tyrosine phosphorylation of PLCγ in response to 2B4 stimulation in mouse NK cells was not sufficiently marked for detection in our assays.

Transfection experiments provided evidence that Src family kinases, in particular Fyn, were responsible for phosphorylation of the C-terminal tyrosines of EAT-2. This notion was also consistent with the fact that the tyrosines are located in typical consensus sequences for phosphorylation by Src kinases (Songyang et al., 1994a, 1995). Co-immunoprecipitation experiments and in vitro binding studies also supported the idea that the interaction between the C-terminal tyrosines of EAT-2 and PLCγ was direct. Moreover, it was dependent on phosphorylation of Y127, which bound to the N-terminal SH2 domain of PLCγ. The sequence surrounding phosphorylated Y127, pYVDV (where pY is phosphotyrosine, V is valine, and D is aspartic acid), is a typical binding site for the PLCγ SH2 domain (consensus sequence pY[V/I/L][E/D][L/I/V], where I is isoleucine, L is leucine, and E is glutamic acid; Songyang et al., 1993).

Although Y127 played a pivotal role in the function of EAT-2, it is noteworthy that, in mice and other nonprimate species, EAT-2 contains an additional tyrosine in the tail, Y120. This tyrosine is located in a conserved sequence (pYENT in the mouse, where N is asparagine and T is threonine), which represents a typical binding site for signaling molecules like Grb-2 and 3BP2 (Songyang et al., 1994b). Hence, in these species, EAT-2 may mediate additional signals via Y120. It is also possible that, in species lacking Y120, EAT-2 couples to these effectors via another sequence. Additional studies are needed to examine these possibilities.

One surprising observation was that treatment of NK cells with the Ca^{2+} chelator, BAPTA-AM, resulted in prominent decrease in 2B4-evoked Erk activation. In contrast, the MEK1 inhibitor PD98059 caused a minimal compromise in Erk activation. Combined, these data suggested that Ca^{2+}, rather than MEK1, was primarily responsible for activation of Erk in response to PLCγ activation. These findings were reminiscent of results recently obtained in B cells (Limnander et al., 2011). In immature B cells, PLCγ-dependent Ca^{2+} fluxes led to Erk activation via a PKC (protein kinase C)-δ and Ras-GRP (guanyl nucleotide-releasing protein)-1–dependent mechanism. An analogous mechanism may underlie the role of Ca^{2+} in 2B4-triggered Erk activation in NK cells.

Another unexpected finding was that, in mouse NK cells, the C-terminal tyrosines were needed not only to promote the activating effect of 2B4 but also to prevent the inhibitory impact of 2B4. Because the C-terminal tyrosines were not needed for EAT-2 to associate with 2B4, these findings implied that the signals mediated by the C-terminal tyrosines were responsible for prevention of inhibition. This is unlike the situation with SAP, in which the signaling motif (R78) was not needed for prevention of inhibition (Dong et al., 2012). Such a disparity suggests that SAP and EAT-2 prevent the inhibitory function of SLAM family receptors by distinct mechanisms. SAP may physically interfere with coupling of SLAM family receptors to inhibitory effectors through a natural blocking effect, as previously suggested (Sayos et al., 1998; Dong et al., 2012). In contrast, EAT-2 may mediate signals that inactivate or antagonize the inhibitory effectors of SLAM family receptors.

SAP stimulates NK cell activation by promoting conjugate formation between NK cells and target cells (Dong et al., 2012). We observed herein that EAT-2 did not augment conjugate formation. This was seen both in mouse NK cells and in YT-S cells. The lack of a stimulating effect of EAT-2 on conjugate formation was in agreement with the absence of effect on Vav-1, which likely mediates the effect of SAP on conjugate formation (Dong et al., 2012). Confocal microscopy studies provided indication that EAT-2 accelerated the effector phase of NK cell activation. Indeed, in YT-S cells, EAT-2 enhanced the proportions of conjugates having MTOCs and granules polarized toward the NK cell synapse. Fewer conjugates exhibited nonpolarized MTOCs or granules, or had a lack of polymerized actin at the NK cell synapse. This effect was absolutely dependent on Y127. It was also

consistent with the impact of EAT-2 in mouse NK cells, in which WT EAT-2, but not EAT-2 Y120,127F, enhanced CD107a exposure. Moreover, experiments with pharmacological inhibitors suggested that it was mediated by the ability of EAT-2 to promote Ca^{2+} fluxes. However, an effect of the Erk pathway was possible, given that inhibition of Ca^{2+} fluxes also prevented Erk activation.

In summary, our data showed that EAT-2 promotes NK cell activation by molecular and cellular mechanisms distinct from those used by SAP. EAT-2 functions through Y127-dependent recruitment of PLCγ, which evokes Ca^{2+} fluxes and Erk activation. These signals enable faster polarization of MTOCs and cytotoxic granules toward the NK cell synapse. This ability of EAT-2 and SAP to couple SLAM family receptors to different signaling pathways and cellular effects likely explains their complementary roles in NK cell activation. It permits SLAM family receptors to mediate a broader range of signals and effects, and to be more efficient at activating NK cells.

Given that EAT-2 strengthens the activating function of SLAM family receptors in NK cells, it may be intriguing that other lymphocytes expressing SAP, in particular T cells, do not express EAT-2 (Roncagalli et al., 2005). Perhaps this distinction reflects the fact that, in T cells, activation is primarily driven by the antigen receptor and the co-receptors CD4 and CD8. In this context, SLAM family receptors may not need to mediate strong signals. In fact, the presence of EAT-2 could have deleterious consequences in T cells, perhaps by enabling antigen receptor-independent signals that were too strong. Nonetheless, it is worth pointing out that some T cells, including activated $V\gamma5^+$ intraepithelial lymphocytes, may express high levels of EAT-2 (www.immgen.org). The possibility that EAT-2 contributes to the innate-like characteristics of these T cells deserves consideration.

MATERIALS AND METHODS

Mice. To generate a mouse strain in which Y120 and Y127 of EAT-2 were replaced by phenylalanines (*Sh2d1b1*^{Y120,127F} mouse), the targeting vector depicted in Fig. 3 A was created. In brief, this construct contained a 4.5-kb 5′ arm that replaced the codon for Y120 (TAT) by TTT, which codes for phenylalanine. This codon is located in exon 3. The construct also possessed a 3-kb 3′ arm that changed the codon for Y127 (TAT) to TTC, which also codes for phenylalanine. The codon for Y127 is in exon 4. In addition, a silent mutation creating an EcoRI site (GAATTC) for screening was introduced at this site. The construct also encompassed the neomycin resistance (*neo*) marker, which was flanked by *frt* sites. After linearization with NotI, the construct was transfected in C57BL/6-derived Bruce 4 embryonic stem cells. Cells were selected in the presence of G418 and clones showing homologous recombination were identified by Southern blotting. Clones containing both the Y120F and the Y127F mutations were identified by sequencing of PCR-generated fragments containing exons 3 and 4. They were then injected into blastocysts and chimeric mice were used for germ line transmission. The *neo* marker was eliminated by breeding mice with a transgenic mouse expressing the Flpe recombinase (B6.SJL-Tg(ACTFLPe)9205Dym/J; The Jackson Laboratory; Rodríguez et al., 2000). Mice were then screened by PCR, using oligonucleotide primers at the positions depicted in Fig. 3 A. C57BL/6 mice lacking EAT-2 or SAP were described previously (Al-Alem et al., 2005; Dong et al., 2012). SAP-deficient mice were provided by L. Yin (International Agency for Research on Cancer, Lyon, France). In all experiments, littermates were used as WT controls. WT C57BL/6 mice were obtained from The Jackson Laboratory. Animal experimentation was approved by the Animal Care Committee of IRCM and performed in accordance with the guidelines of the Canadian Council of Animal Care.

cDNAs and plasmids. cDNAs coding for human EAT-2 (WT or Y127F), mouse EAT-2 (WT; Y120F; Y127F; Y120,127F; R54L; R54L,Y120F; and R54L,Y127F), FLAG-tagged mouse EAT-2, human CD48, and PLC-γ1 were generated by PCR and verified by sequencing. Those encoding mouse 2B4, mouse CRACC, various PTKs, and an SH2 domain–deleted variant of Fyn were reported previously (Cao et al., 1998; Chen et al., 2006; Cruz-Munoz et al., 2009). For expression in YT-S, K562, and HeLa, cDNAs were usually cloned in the retroviral vector pFB-GFP, which also encodes GFP. For expression in Cos-1 cells, cDNAs were cloned in the vector pXM319.

Cells. For real-time PCR analyses, cells were purified by cell sorting. In brief, NKPs (Lin^-, $CD122^+$, $NK1.1^-$, and $CD49b^-$), iNK cells (Lin^-, $CD122^+$, $NK1.1^+$, and $CD49b^-$), and mNK cells (Lin^-, $CD122^+$, $NK1.1^+$, and $CD49b^+$) were obtained from bone marrow of C57BL/6 mice using antibodies directed against CD19, Ter-119, B220, CD122, NK1.1, and CD49b, as described elsewhere (Ramirez et al., 2012). Splenic mNK cells were isolated by staining with antibodies against CD122, NK.1.1, and CD49b, whereas splenic B cells were obtained by staining with antibodies directed against B220 and CD19. In all cases, cell purity was >90%. Freshly isolated splenic NK cells from poly I:C–primed mice and spleen-derived LAK cells were generated as outlined elsewhere (Dong et al., 2009). RMA-S (lymphoma), YAC-1 (thymoma), and B16 (melanoma) expressing or not SLAM family ligands were described elsewhere (Dong et al., 2009, 2012). Control B16 cells expressed GFP alone. YT-S, K562, HeLa, and Cos-1 cells were reported elsewhere (Chen et al., 2006; Cruz-Munoz et al., 2009). YT-S cells expressing GFP alone or in combination with WT or Y127F human EAT-2 were generated by retroviral infection, using the retroviral vector pFB-GFP. Transduced cells were sorted for expression of GFP. K562 or HeLa derivatives expressing human CD48 or mouse CRACC were generated in a similar way. Cos-1 cell transfections were performed as outlined previously (Latour et al., 1997).

Antibodies. Antibodies recognizing CD19 (mAb 1D3), Ter-119 (mAb Ter119), B220 (mAb RA3-6B2), CD122 (mAb TM-b1), NK1.1 (mAb PK136), CD49b (mAb DX5), human 2B4 (mAb C1.7), human CD48 (mAb TÜ145), mouse 2B4 (mAb 2B4), mouse CD48 (mAb HM48-1), CD3 (mAb 145-2C11), CD11b (mAb M1/70), CD27 (LG.7F9), IFN-γ (mAb XMG1.2), CD107a (mAb eBio 1D4B), CD16 (mAb 2.4G2), Ly49D (mAb 4E5), Ly49H (mAb 3D10), and Ly49C/I/F/H (mAb 14B11), as well as isotype controls, were purchased from eBioscience or BD. Anti–phospho-Erk (pT202pY204; mAb E10), anti–phospho-Akt (pS473; mAb 193H12), and anti-Akt were obtained from Cell Signaling Technology, and antibodies directed against phosphotyrosine (mAb 4G10) or Erk were from Millipore. Anti-FLAG mAb M2 was obtained from Sigma-Aldrich. Antibodies against mouse EAT-2 (mAb 8F12), SAP (mAb 1A9), mouse Ly-9, mouse Ly108, mouse CD84, mouse SLAM, and mouse CRACC were produced in our laboratories (Roncagalli et al., 2005; Veillette et al., 2008; Zhong and Veillette, 2008; Cruz-Munoz et al., 2009). Monoclonal antibodies against human EAT-2 (mAb 10F7) were generated by immunizing mice with the full-length human EAT-2 protein (COVALAB). Polyclonal rabbit antibodies against human 2B4 were provided by E. Long (National Institutes of Health, Rockville, MD). Those against Fyn, Vav-1, SHIP-1, and c-Cbl were described elsewhere (Chen et al., 2006). Antibodies against PLCγ-1 and PLCγ-2 were purchased from Santa Cruz Biotechnology, Inc.

Quantitative real-time PCR. RNA was purified with the RNeasy micro kit (QIAGEN), and reverse transcribed using the SensiScript kit (QIAGEN) and oligo (dT) primers (Ambion). PCR reactions were performed using single-stranded cDNAs, gene-specific primers, and the PerfeCTa SYBR Green Supermix (Quanta), according to the manufacturer's instructions. Real-time PCR was performed in duplicates, and fluorometric data were collected at the annealing step of each cycle, using the ViiA Real-Time PCR

system (Life Technologies). A dissociation curve was obtained at the end of 40 cycles to confirm specificity of amplification. Expression is reported as Δ cross threshold (ΔCT), which is relative to *Gapdh* mRNA and normalized to values for LAK cells. The sense and antisense PCR primers were: *Sh2d1a* (SAP), 5′-ACAGAAACAGGTTCTTGGAGTG-3′ and 5′-GCATTCAGGCAGATATCAGAATC-3′; *Sh2d1b1* (EAT-2), 5′-CAGGATAGAGACTAATGCTCATAC-3′ and 5′-CAGGATAGAGACTAATGCTCATAC-3′; *Sh2d1b2* (ERT), 5′-AGGATAGAGACTGAGCCCAG-3′ and 5′-CTGGACAGAAGCCGCTTCCTC-3′; and *Gapdh*, 5′-AAATGGTGAAGGTCGGTGTG-3′ and 5′-GCTCTGGAAGATGGTGATG-3′.

Sequence and RNA expression databases. Amino acid sequences of EAT-2 from different species were obtained by searching the public database PROTEIN at the NCBI website. Alignments were done using ClustalW2 online software from the EBI website and results were edited with BioEdit software v7.2.1, Ibis BioScience. Microarray data assembled by the Immunological Genome Project Consortium (ImmGen) were downloaded from their website (www.immgen.org). Data are shown as reported.

NK cell assays. Poly I:C–activated ex vivo NK cells or IL-2–expanded NK cells were generated as outlined previously (Dong et al., 2009, 2012). NK cell–mediated cytotoxicity and IFN-γ production were assayed as detailed elsewhere (Dong et al., 2009, 2012).

Antibody-mediated cell stimulation. Antibody-mediated stimulation of 2B4, CD16, or both on YT-S cells or mouse NK cells was performed as explained elsewhere (Chen et al., 2006; Dong et al., 2009, 2012). Cells were then processed for immunoprecipitation, immunoblotting, or Ca^{2+} fluxes, which have been previously described (Chen et al., 2006; Dong et al., 2009, 2012).

Immunoprecipitations and immunoblots. Immunoprecipitations and immunoblots were performed as reported (Veillette et al., 1988).

Pharmacological inhibitors. The Ca^{2+} chelator BAPTA-AM and the MEK1 inhibitor PD98059 were purchased from Merck. They were dissolved in DMSO. To establish the optimal concentration of the compounds for our experiments, YT-S cells were incubated for 30 min with increasing amounts of the compounds in culture medium. 2B4-triggered intracellular Ca^{2+} fluxes or Erk activation was then examined. The lower concentration needed for maximally inhibiting these responses, without compromising cell viability, was chosen. These concentrations were: BAPTA-AM, 20 μM; and PD98059, 100 μM. PD98059 failed to cause complete inhibition of Erk1/2, even at a concentration of 100 μM. In all experiments, compounds were added 30 min before the functional or biochemical assays. Cell viability was monitored by trypan blue exclusion or flow cytometry, using forward side channel (FSC) and side scatter channel (SSC) analysis.

Peptide and fusion protein binding experiments. Biotinylated peptides encompassing the 29–amino acid C-terminal sequence of human or mouse EAT-2, phosphorylated or not at Y120, Y127, or both, were synthesized by the W.M. Keck Facility (Yale University, New Haven, CT). Peptides were dissolved in DMSO at a concentration of 10 μg/μl and coupled to Neutravidin agarose beads (Thermo Fisher Scientific). Beads were then incubated with the indicated cell lysates for 90 min at 4°C. They were extensively washed and association with PLCγ was detected by immunoblotting. GST fusion proteins encompassing various domains were produced in bacteria, as detailed elsewhere (Roncagalli et al., 2005). They were then incubated with lysates of HeLa cells expressing cDNAs encoding FLAG-tagged mouse EAT-2 in the presence of SH2 domain-deleted Fyn, or with immobilized EAT-2 peptides. After several washes, binding was detected by immunoblotting.

Conjugate formation assays. YT-S cells were first labeled on ice by incubation with Alexa Fluor 647–conjugated anti–human CD335 mAb 9E2 (BioLegend), which recognizes NKp46. Although NKp46 is expressed on YT-S, it is not functional (our unpublished results). K562 cells were labeled in a similar way, using PE-conjugated anti–human CD71 mAb CY1G4 (BioLegend). After washing the unbound antibodies, cells were resuspended at a concentration of 2×10^6 cells per ml and conjugate formation was analyzed as previously described (Dong et al., 2012).

Confocal microscopy. K562 cells were first stained with the Cell Tracker Violet dye (Life Technologies), according to the manufacturer's instructions. After washing, cells were allowed to recover by incubation in culture medium for at least 10 min. YT-S cells and K562 cells were then mixed at a 2:1 ratio in serum-free culture medium and incubated for 10 min at 37°C to allow conjugate formation. The suspension was subsequently transferred to poly-L-lysine–coated coverslips and incubated an additional 5 min at 37°C for attachment. Cells were then fixed and permeabilized in PBS containing 4% formaldehyde and 0.1% saponin. After that, they were washed twice with PBS containing 0.1% saponin and blocked for 30 min in PBS supplemented with 5% mouse serum. They were washed again and incubated for 1 h with biotinylated anti-tubulin mAb 236–10501 (Life Technologies). After further washing, cells were incubated for 1 h with Alexa Fluor 647–coupled anti-perforin mAb dG9 (BioLegend), Brilliant violet 605–coupled streptavidin (BioLegend), and Alexa Fluor 546–coupled phalloidin (Invitrogen). After an additional wash, coverslips were mounted over glass slides using fluorescent mounting medium (Dako). Data were acquired using a laser-scanning microscope LSM-710 (Carl Zeiss). Only conjugates in which one YT-S cell was coupled to one K562 cell were analyzed. At least 100 different conjugates were analyzed for each cell type or condition. Conjugate stages were defined as: 0, conjugates lacking actin polymerization, and MTOC and granule polarization; 1, conjugates with polymerized actin, but devoid of MTOC and granule polarization; 2, conjugates where MTOC and granules have partially migrated toward the synapse; and 3, conjugates where MTOC and granules have fully migrated toward the synapse.

CD107a exposure. To measure induction of CD107a expression at the cell surface, splenocytes (2×10^6) from poly I:C–primed mice were cultured with the same number of RMA-S cells, GolgiStop (BD), and Alexa Fluor 488–conjugated anti-CD107a antibody. After 6 h, cells were harvested and analyzed by flow cytometry. NK cells were identified by gating on $NK1.1^+CD3^-$ cells. As control, cells were stimulated with a combination of PMA plus ionomycin.

Statistical analyses. For statistical analyses of cytotoxicity and IFN-γ production, paired Student's *t* tests (two-tailed) were performed. For statistical comparison of the relative distribution of YT-S:K562 conjugates in the various stages of cytotoxicity, data for individual cell populations were compared using the Pearson correlation coefficient (*r*). All statistics were calculated using Prism 6 (GraphPad Software).

We thank the members of our laboratory for discussions. We also acknowledge Eric Long for the anti–human 2B4 serum and Luo Yin for the SAP-deficient mouse. We thank Kevin Ramirez and Barbara Kee for advice on purification of NK cell subsets.

This work was supported by grants from the Canadian Institutes of Health Research and the Canadian Cancer Society Research Institute (CCSRI) to A. Veillette. L.-A. Pérez-Quintero and H. Guo were recipients of Studentships from the Clinical Research Institute of Montreal and McGill University, respectively. R. Roncagalli was recipient of a Studentship from CCSRI. A. Veillette holds the Canada Research Chair in Signaling in the Immune System.

The authors declare no competing financial interests.

Submitted: 25 September 2013
Accepted: 4 March 2014

REFERENCES

Al-Alem, U., C. Li, N. Forey, F. Relouzat, M.C. Fondanèche, S.V. Tavtigian, Z.Q. Wang, S. Latour, and L. Yin. 2005. Impaired Ig class switch in mice deficient for the X-linked lymphoproliferative disease gene Sap. *Blood*. 106:2069–2075. http://dx.doi.org/10.1182/blood-2004-07-2731

Bottino, C., M. Falco, S. Parolini, E. Marcenaro, R. Augugliaro, S. Sivori, E. Landi, R. Biassoni, L.D. Notarangelo, L. Moretta, and A. Moretta. 2001.

NTB-A, a novel SH2D1A-associated surface molecule contributing to the inability of natural killer cells to kill Epstein-Barr virus–infected B cells in X-linked lymphoproliferative disease. *J. Exp. Med.* 194:235–246. http://dx.doi.org/10.1084/jem.194.3.235

Bryceson, Y.T., and E.O. Long. 2008. Line of attack: NK cell specificity and integration of signals. *Curr. Opin. Immunol.* 20:344–352. http://dx.doi.org/10.1016/j.coi.2008.03.005

Calpe, S., E. Erdos, G. Liao, N. Wang, S. Rietdijk, M. Simarro, B. Scholtz, J. Mooney, C.H. Lee, M.S. Shin, et al. 2006. Identification and characterization of two related murine genes, Eat2a and Eat2b, encoding single SH2-domain adapters. *Immunogenetics*. 58:15–25. http://dx.doi.org/10.1007/s00251-005-0056-3

Cannons, J.L., S.G. Tangye, and P.L. Schwartzberg. 2011. SLAM family receptors and SAP adaptors in immunity. *Annu. Rev. Immunol.* 29:665–705. http://dx.doi.org/10.1146/annurev-immunol-030409-101302

Cao, M.Y., M. Huber, N. Beauchemin, J. Famiglietti, S.M. Albelda, and A. Veillette. 1998. Regulation of mouse PECAM-1 tyrosine phosphorylation by the Src and Csk families of protein-tyrosine kinases. *J. Biol. Chem.* 273:15765–15772. http://dx.doi.org/10.1074/jbc.273.25.15765

Caraux, A., N. Kim, S.E. Bell, S. Zompi, T. Ranson, S. Lesjean-Pottier, M.E. Garcia-Ojeda, M. Turner, and F. Colucci. 2006. Phospholipase C-γ2 is essential for NK cell cytotoxicity and innate immunity to malignant and virally infected cells. *Blood*. 107:994–1002. http://dx.doi.org/10.1182/blood-2005-06-2428

Chan, B., A. Lanyi, H.K. Song, J. Griesbach, M. Simarro-Grande, F. Poy, D. Howie, J. Sumegi, C. Terhorst, and M.J. Eck. 2003. SAP couples Fyn to SLAM immune receptors. *Nat. Cell Biol.* 5:155–160. http://dx.doi.org/10.1038/ncb920

Chen, R., F. Relouzat, R. Roncagalli, A. Aoukaty, R. Tan, S. Latour, and A. Veillette. 2004. Molecular dissection of 2B4 signaling: implications for signal transduction by SLAM-related receptors. *Mol. Cell. Biol.* 24:5144–5156. http://dx.doi.org/10.1128/MCB.24.12.5144-5156.2004

Chen, R., S. Latour, X. Shi, and A. Veillette. 2006. Association between SAP and FynT: Inducible SH3 domain-mediated interaction controlled by engagement of the SLAM receptor. *Mol. Cell. Biol.* 26:5559–5568. http://dx.doi.org/10.1128/MCB.00357-06

Clarkson, N.G., and M.H. Brown. 2009. Inhibition and activation by CD244 depends on CD2 and phospholipase C-γ1. *J. Biol. Chem.* 284:24725–24734. http://dx.doi.org/10.1074/jbc.M109.028209

Clarkson, N.G., S.J. Simmonds, M.J. Puklavec, and M.H. Brown. 2007. Direct and indirect interactions of the cytoplasmic region of CD244 (2B4) in mice and humans with FYN kinase. *J. Biol. Chem.* 282:25385–25394. http://dx.doi.org/10.1074/jbc.M704483200

Cruz-Munoz, M.E., Z. Dong, X. Shi, S. Zhang, and A. Veillette. 2009. Influence of CRACC, a SLAM family receptor coupled to the adaptor EAT-2, on natural killer cell function. *Nat. Immunol.* 10:297–305. http://dx.doi.org/10.1038/ni.1693

Detre, C., M. Keszei, X. Romero, G.C. Tsokos, and C. Terhorst. 2010. SLAM family receptors and the SLAM-associated protein (SAP) modulate T cell functions. *Semin. Immunopathol.* 32:157–171. http://dx.doi.org/10.1007/s00281-009-0193-0

Dong, Z., and A. Veillette. 2010. How do SAP family deficiencies compromise immunity? *Trends Immunol.* 31:295–302. http://dx.doi.org/10.1016/j.it.2010.05.008

Dong, Z., M.E. Cruz-Munoz, M.C. Zhong, R. Chen, S. Latour, and A. Veillette. 2009. Essential function for SAP family adaptors in the surveillance of hematopoietic cells by natural killer cells. *Nat. Immunol.* 10:973–980. http://dx.doi.org/10.1038/ni.1763

Dong, Z., D. Davidson, L.A. Pérez-Quintero, T. Kurosaki, W. Swat, and A. Veillette. 2012. The adaptor SAP controls NK cell activation by regulating the enzymes Vav-1 and SHIP-1 and by enhancing conjugates with target cells. *Immunity*. 36:974–985. http://dx.doi.org/10.1016/j.immuni.2012.03.023

Dupré, L., G. Andolfi, S.G. Tangye, R. Clementi, F. Locatelli, M. Aricò, A. Aiuti, and M.G. Roncarolo. 2005. SAP controls the cytolytic activity of $CD8^+$ T cells against EBV-infected cells. *Blood*. 105:4383–4389. http://dx.doi.org/10.1182/blood-2004-08-3269

Hislop, A.D., U. Palendira, A.M. Leese, P.D. Arkwright, P.S. Rohrlich, S.G. Tangye, H.B. Gaspar, A.C. Lankester, A. Moretta, and A.B. Rickinson. 2010. Impaired Epstein-Barr virus–specific $CD8^+$ T-cell function in X-linked lymphoproliferative disease is restricted to SLAM family–positive B-cell targets. *Blood*. 116:3249–3257. http://dx.doi.org/10.1182/blood-2009-09-238832

Kageyama, R., J.L. Cannons, F. Zhao, I. Yusuf, C. Lao, M. Locci, P.L. Schwartzberg, and S. Crotty. 2012. The receptor Ly108 functions as a SAP adaptor-dependent on-off switch for T cell help to B cells and NKT cell development. *Immunity*. 36:986–1002. http://dx.doi.org/10.1016/j.immuni.2012.05.016

Lanier, L.L. 2005. NK cell recognition. *Annu. Rev. Immunol.* 23:225–274. http://dx.doi.org/10.1146/annurev.immunol.23.021704.115526

Latour, S., M. Fournel, and A. Veillette. 1997. Regulation of T-cell antigen receptor signalling by Syk tyrosine protein kinase. *Mol. Cell. Biol.* 17:4434–4441.

Latour, S., G. Gish, C.D. Helgason, R.K. Humphries, T. Pawson, and A. Veillette. 2001. Regulation of SLAM-mediated signal transduction by SAP, the X-linked lymphoproliferative gene product. *Nat. Immunol.* 2:681–690. http://dx.doi.org/10.1038/90615

Latour, S., R. Roncagalli, R. Chen, M. Bakinowski, X. Shi, P.L. Schwartzberg, D. Davidson, and A. Veillette. 2003. Binding of SAP SH2 domain to FynT SH3 domain reveals a novel mechanism of receptor signalling in immune regulation. *Nat. Cell Biol.* 5:149–154. http://dx.doi.org/10.1038/ncb919

Limnander, A., P. Depeille, T.S. Freedman, J. Liou, M. Leitges, T. Kurosaki, J.P. Roose, and A. Weiss. 2011. STIM1, PKC-δ and RasGRP set a threshold for proapoptotic Erk signaling during B cell development. *Nat. Immunol.* 12:425–433. http://dx.doi.org/10.1038/ni.2016

Morra, M., J. Lu, F. Poy, M. Martin, J. Sayos, S. Calpe, C. Gullo, D. Howie, S. Rietdijk, A. Thompson, et al. 2001. Structural basis for the interaction of the free SH2 domain EAT-2 with SLAM receptors in hematopoietic cells. *EMBO J.* 20:5840–5852. http://dx.doi.org/10.1093/emboj/20.21.5840

Orange, J.S. 2008. Formation and function of the lytic NK-cell immunological synapse. *Nat. Rev. Immunol.* 8:713–725. http://dx.doi.org/10.1038/nri2381

Palendira, U., C. Low, A. Chan, A.D. Hislop, E. Ho, T.G. Phan, E. Deenick, M.C. Cook, D.S. Riminton, S. Choo, et al. 2011. Molecular pathogenesis of EBV susceptibility in XLP as revealed by analysis of female carriers with heterozygous expression of SAP. *PLoS Biol.* 9:e1001187. http://dx.doi.org/10.1371/journal.pbio.1001187

Palendira, U., C. Low, A.I. Bell, C.S. Ma, R.J. Abbott, T.G. Phan, D.S. Riminton, S. Choo, J.M. Smart, V. Lougaris, et al. 2012. Expansion of somatically reverted memory $CD8^+$ T cells in patients with X-linked lymphoproliferative disease caused by selective pressure from Epstein-Barr virus. *J. Exp. Med.* 209:913–924. http://dx.doi.org/10.1084/jem.20112391

Parolini, S., C. Bottino, M. Falco, R. Augugliaro, S. Giliani, R. Franceschini, H.D. Ochs, H. Wolf, J.Y. Bonnefoy, R. Biassoni, et al. 2000. X-linked lymphoproliferative disease. 2B4 molecules displaying inhibitory rather than activating function are responsible for the inability of natural killer cells to kill Epstein-Barr virus-infected cells. *J. Exp. Med.* 192:337–346. http://dx.doi.org/10.1084/jem.192.3.337

Qi, H., J.L. Cannons, F. Klauschen, P.L. Schwartzberg, and R.N. Germain. 2008. SAP-controlled T-B cell interactions underlie germinal centre formation. *Nature*. 455:764–769. http://dx.doi.org/10.1038/nature07345

Ramirez, K., K.J. Chandler, C. Spaulding, S. Zandi, M. Sigvardsson, B.J. Graves, and B.L. Kee. 2012. Gene deregulation and chronic activation in natural killer cells deficient in the transcription factor ETS1. *Immunity*. 36:921–932. http://dx.doi.org/10.1016/j.immuni.2012.04.006

Raulet, D.H. 2003. Roles of the NKG2D immunoreceptor and its ligands. *Nat. Rev. Immunol.* 3:781–790. http://dx.doi.org/10.1038/nri1199

Regunathan, J., Y. Chen, S. Kutlesa, X. Dai, L. Bai, R. Wen, D. Wang, and S. Malarkannan. 2006. Differential and nonredundant roles of phospholipase Cγ2 and phospholipase Cγ1 in the terminal maturation of NK cells. *J. Immunol.* 177:5365–5376.

Rodríguez, C.I., F. Buchholz, J. Galloway, R. Sequerra, J. Kasper, R. Ayala, A.F. Stewart, and S.M. Dymecki. 2000. High-efficiency deleter mice show that FLPe is an alternative to Cre-loxP. *Nat. Genet.* 25:139–140. http://dx.doi.org/10.1038/75973

Roncagalli, R., J.E. Taylor, S. Zhang, X. Shi, R. Chen, M.E. Cruz-Munoz, L. Yin, S. Latour, and A. Veillette. 2005. Negative regulation of natural killer cell function by EAT-2, a SAP-related adaptor. *Nat. Immunol.* 6:1002–1010. http://dx.doi.org/10.1038/ni1242

Sayos, J., C. Wu, M. Morra, N. Wang, X. Zhang, D. Allen, S. van Schaik, L. Notarangelo, R. Geha, M.G. Roncarolo, et al. 1998. The X-linked lymphoproliferative-disease gene product SAP regulates signals induced through the co-receptor SLAM. *Nature*. 395:462–469. http://dx.doi.org/10.1038/26683

Songyang, Z., S.E. Shoelson, M. Chaudhuri, G. Gish, T. Pawson, W.G. Haser, F. King, T. Roberts, S. Ratnofsky, R.J. Lechleider, et al. 1993. SH2 domains recognize specific phosphopeptide sequences. *Cell.* 72:767–778. http://dx.doi.org/10.1016/0092-8674(93)90404-E

Songyang, Z., S. Blechner, N. Hoagland, M.F. Hoekstra, H. Piwnica-Worms, and L.C. Cantley. 1994a. Use of an oriented peptide library to determine the optimal substrates of protein kinases. *Curr. Biol.* 4:973–982. http://dx.doi.org/10.1016/S0960-9822(00)00221-9

Songyang, Z., S.E. Shoelson, J. McGlade, P. Olivier, T. Pawson, X.R. Bustelo, M. Barbacid, H. Sabe, H. Hanafusa, T. Yi, et al. 1994b. Specific motifs recognized by the SH2 domains of Csk, 3BP2, fps/fes, GRB-2, HCP, SHC, Syk, and Vav. *Mol. Cell. Biol.* 14:2777–2785. http://dx.doi.org/10.1128/MCB.14.4.2777

Songyang, Z., K.L. Carraway III, M.J. Eck, S.C. Harrison, R.A. Feldman, M. Mohammadi, J. Schlessinger, S.R. Hubbard, D.P. Smith, C. Eng, et al. 1995. Catalytic specificity of protein-tyrosine kinases is critical for selective signalling. *Nature*. 373:536–539. http://dx.doi.org/10.1038/373536a0

Tassi, I., and M. Colonna. 2005. The cytotoxicity receptor CRACC (CS-1) recruits EAT-2 and activates the PI3K and phospholipase Cγ signaling pathways in human NK cells. *J. Immunol.* 175:7996–8002.

Tassi, I., R. Presti, S. Kim, W.M. Yokoyama, S. Gilfillan, and M. Colonna. 2005. Phospholipase C-γ2 is a critical signaling mediator for murine NK cell activating receptors. *J. Immunol.* 175:749–754.

Thien, C.B., and W.Y. Langdon. 2005. c-Cbl and Cbl-b ubiquitin ligases: substrate diversity and the negative regulation of signalling responses. *Biochem. J.* 391:153–166. http://dx.doi.org/10.1042/BJ20050892

Ting, A.T., L.M. Karnitz, R.A. Schoon, R.T. Abraham, and P.J. Leibson. 1992. Fc gamma receptor activation induces the tyrosine phosphorylation of both phospholipase C (PLC)-gamma 1 and PLC-gamma 2 in natural killer cells. *J. Exp. Med.* 176:1751–1755. http://dx.doi.org/10.1084/jem.176.6.1751

Veillette, A. 2010. SLAM-family receptors: immune regulators with or without SAP-family adaptors. *Cold Spring Harb. Perspect. Biol.* 2:a002469. http://dx.doi.org/10.1101/cshperspect.a002469

Veillette, A., M.A. Bookman, E.M. Horak, and J.B. Bolen. 1988. The CD4 and CD8 T cell surface antigens are associated with the internal membrane tyrosine-protein kinase p56lck. *Cell.* 55:301–308. http://dx.doi.org/10.1016/0092-8674(88)90053-0

Veillette, A., S. Zhang, X. Shi, Z. Dong, D. Davidson, and M.C. Zhong. 2008. SAP expression in T cells, not in B cells, is required for humoral immunity. *Proc. Natl. Acad. Sci. USA.* 105:1273–1278. http://dx.doi.org/10.1073/pnas.0710698105

Vivier, E., E. Tomasello, M. Baratin, T. Walzer, and S. Ugolini. 2008. Functions of natural killer cells. *Nat. Immunol.* 9:503–510. http://dx.doi.org/10.1038/ni1582

Wang, N., S. Calpe, J. Westcott, W. Castro, C. Ma, P. Engel, J.D. Schatzle, and C. Terhorst. 2010. Cutting edge: The adapters EAT-2A and -2B are positive regulators of CD244- and CD84-dependent NK cell functions in the C57BL/6 mouse. *J. Immunol.* 185:5683–5687. http://dx.doi.org/10.4049/jimmunol.1001974

Zhao, F., J.L. Cannons, M. Dutta, G.M. Griffiths, and P.L. Schwartzberg. 2012. Positive and negative signaling through SLAM receptors regulate synapse organization and thresholds of cytolysis. *Immunity.* 36:1003–1016. http://dx.doi.org/10.1016/j.immuni.2012.05.017

Zhong, M.C., and A. Veillette. 2008. Control of T lymphocyte signaling by Ly108, a signaling lymphocytic activation molecule family receptor implicated in autoimmunity. *J. Biol. Chem.* 283:19255–19264. http://dx.doi.org/10.1074/jbc.M800209200